Computational Motor Control: Redundancy and Invariance

Emmanuel Guigon,[1] Pierre Baraduc,[2] and Michel Desmurget[3]

[1]*Institut National de la Santé et de la Recherche Médicale (INSERM) U742, Action Neuroimagerie Modelisation, Université Pierre et Marie Curie, Paris;* [2]*INSERM U534, Space and Action; and* [3]*INSERM U371, Brain and Vision Research, Bron, France*

Guigon E, Baraduc P, Desmurget M. Computational motor control: redundancy and invariance. *J Neurophysiol* 97: 331–347, 2007. First published September 27, 2006; doi:10.1152/jn.00290.2006. The nervous system controls the behavior of complex kinematically redundant biomechanical systems. How it computes appropriate commands to generate movements is unknown. Here we propose a model based on the assumption that the nervous system: *1*) processes static (e.g., gravitational) and dynamic (e.g., inertial) forces separately; *2*) calculates appropriate dynamic controls to master the dynamic forces and progress toward the goal according to principles of optimal feedback control; *3*) uses the size of the dynamic commands (effort) as an optimality criterion; and *4*) can specify movement duration from a given level of effort. The model was used to control kinematic chains with 2, 4, and 7 degrees of freedom [planar shoulder/elbow, three-dimensional (3D) shoulder/elbow, 3D shoulder/elbow/wrist] actuated by pairs of antagonist muscles. The muscles were modeled as second-order nonlinear filters and received the dynamics commands as inputs. Simulations showed that the model can quantitatively reproduce characteristic features of pointing and grasping movements in 3D space, i.e., trajectory, velocity profile, and final posture. Furthermore, it accounted for amplitude/duration scaling and kinematic invariance for distance and load. These results suggest that motor control could be explained in terms of a limited set of computational principles.

INTRODUCTION

When we move our limbs to execute a motor task, we generally have many more degrees of freedom (DOF) than necessary to fulfill the requirements of the task. In a typical situation, unconstrained point-to-point arm movements involve 7 DOF for moving in a three-dimensional (3D) space. If movements are to occur in a plane, such as in a handwriting task, the physical constraint of contact still leaves infinitely many solutions to the problem of writing a letter. The coordination of kinematically redundant systems was first formulated by Bernstein (1967) as the *DOF problem*. The main difficulty of Bernstein's problem is that the nervous system must conciliate two apparently conflicting abilities. On the one hand, each individual realization of a motor goal results from the choice of one among an infinite number of motor patterns. On the other hand, there is no univocal relationship between motor goals and motor patterns, a property first noted to be central to the functioning of motor systems by Lashley (1933), which he called *motor equivalence*. For instance, the nervous system can preserve a common kinematic pattern for executing a movement while varying the moving effector, the angular patterns of motion, or underlying muscular activations (Bernstein 1967; Burdet et al. 2001; Gribble et al. 2003; Levin et al. 2003). Solving Bernstein's problem should not only help us under-

stand the origin of this *flexibility*, but also explain how the flexibility coexists with constraints inherent to the functioning of the motor system. For instance, when subjects are free to move, they automatically scale movement duration with movement amplitude and choose a trade-off between movement speed and accuracy (Fitts' law; Fitts 1954). An open question is how motor controllers in the brain solve Bernstein's problem. Here, we first present a computational approach to this problem, i.e., a solution cast in terms of principles. Our goal is to provide a solution based on a restricted number of realistic and well-supported hypotheses. Then we show how these principles apply to the problem of kinematic redundancy.

COMPUTATIONAL APPROACH

Breakthroughs into the understanding of motor functions have generally been brought about by computational studies (Bullock and Grossberg 1988; Feldman and Levin 1995; Flash and Hogan 1985; Harris and Wolpert 1998; Hoff and Arbib 1993; Todorov and Jordan 2002; Uno et al. 1989), i.e., studies that disclose functioning principles independent of brain structures or neural processes. However, since the time of Bernstein and Lashley, no adequate principled approach to kinematic redundancy and motor equivalence has been proposed and the way the nervous system tackles these problems remains mysterious (Gielen et al. 1995). In particular, the line of reasoning based on the separation between trajectory planning and trajectory execution, which attributes motor equivalence to the specification of a desired trajectory in task coordinates and which proposes a solution to redundancy using inverse kinematic transformations, has been seriously questioned (Bullock and Grossberg 1988; Cole and Abbs 1986; Sporns and Edelman 1993; Todorov 2004; Todorov and Jordan 2002). The main argument is that on-line movement corrections act to favor goal achievement rather than the following of a preplanned trajectory.

Principles

The goal of this article is to describe a principled approach that gives a unified account of motor behavior. We propose that motor control is governed by four principles: *1*) *separation*: the nervous system processes dynamic (inertial, velocity-dependent) and static (elastic, gravitational) forces separately; *2*) *optimal feedback control*: there exists an optimal controller for dynamic forces (dynamic controller) that is appropriate for an on-line control of movement, i.e., it is optimal for any initial state of the moving limb; *3*) *maximum efficiency*: the nervous system attempts to reach the goal of the movement defined in the task coordinates with zero error and minimal control

---

signals (these signals are inputs of central descending origin to motoneurons; overall control magnitude is called *effort*; see METHODS); *4) constant effort*: all movements obeying a given set of instructions (e.g., move at preferred speed) are executed with the same level of effort. Maximum efficiency and constant effort are not incompatible. The former principle associates each movement duration to an effort level, i.e., the (minimal) effort of the optimal solution. When duration is not specified, the latter principle prescribes a level of effort used to determine the appropriate duration, i.e., the unique duration associated to this level of effort.

Below, we give a brief rationale for these principles. In the RESULTS section, we show how they are associated to properties of motor behavior.

SEPARATION PRINCIPLE.   There is substantial experimental evidence to support the idea of a separate processing of static and dynamic forces. Previous psychophysical studies showed that velocity profiles remain unchanged when moving in a known constant (Mustard and Lee 1987; Welter and Bobbert 2002) or a known elastic force field (Bock 1990; Flash and Gurevich 1992; Ghez 1979; Gottlieb 1996; Levin et al. 2003; Milner 2002; Rand et al. 2004), but that they are in general modified by time and amplitude scaling in velocity-dependent and inertial fields (Atkeson and Hollerbach 1985; Bock 1990; Gottlieb 1996; Happee 1993; Hatzitaki and McKinley 2001; Ruitenbeek 1984). This property is called *kinematic invariance*. These results show that, if a separation principle holds, it does not apply to any type of forces, but is specific to static forces. Even if some velocity-dependent perturbations have no influence on movement kinematics (Shadmehr and Moussavi 2000; Shadmehr and Mussa-Ivaldi 1994), our reasoning and conclusion remain valid. Electromyographic (EMG) studies revealed additive velocity-independent, tonic and velocity-dependent, phasic components that are related to the generation of antigravity torques and *dynamic* torques, respectively (Buneo et al. 1994; Flanders and Herrmann 1992; see also Farley and Koshland 2000; Milner 2002; Welter and Bobbert 2002). A similar additive combination between a tonic activity, related to the compensation of an external static force, and a phasic, movement-related activity was observed in neurons of primate motor cortex (Kalaska et al. 1989). The experiment of Nishikawa et al. (1999) showed that the terminal posture of 3D redundant movements is independent of movement velocity. Because the relative contribution of antigravity and dynamic torques varies with velocity, optimization of the total torque pattern would predict variations of terminal posture with velocity. This result suggests that dynamic forces are optimized independent of static forces. The study of Kurtzer et al. (2005a) provides further support to the separation principle. These authors showed that adaptation to a multiforce environment composed of a velocity-dependent force and a constant force was well described by a mechanism that processes velocity-dependent force separately from the total applied force. We emphasize that separation of static and dynamic forces is not separation of posture and movement because static forces (gravity, muscular elastic forces) are present during both posture and movement.

OPTIMAL FEEDBACK CONTROL PRINCIPLE.   A solution to kinematic redundancy could likely be found in the framework of optimal control theory, which states that a unique solution to an ill-posed problem can generally be obtained as the solution that corresponds to the minimum of a *cost* function. Because it is well recognized that motor commands are continuously updated by internal feedback loops (review in Desmurget and Grafton 2000), it has been suggested that on-line control of movement is also optimal in the theoretical sense (*optimal feedback control*; Bryson and Ho 1975; Hoff and Arbib 1993; Todorov and Jordan 2002). This means that the control signals are optimal for any boundary conditions, such as following perturbation of the moving limb or changes in target position. The notion that motor control can be viewed as a continuous feedback process was first analyzed by Bullock and Grossberg (1988) and was shown to account for trajectory formation and kinematic invariance.

It is paradoxical that optimal control theory has been repeatedly and successfully used to account for many aspects of motor control (e.g., trajectory formation, muscular redundancy, postural control, locomotion; Anderson and Pandy 2001; Flash and Hogan 1985; Harris and Wolpert 1998; Kuo 1995; Uno et al. 1989), but has rarely been applied to the case of redundant manipulators (Todorov and Jordan 2002). Todorov and Jordan (2002) successfully applied optimal control to a kinematically redundant system. However, this work was limited to the linear case, i.e., a telescopic arm model rather than an articulated arm with a nonlinear dynamics. Also, no direct comparison was provided between experimental data and the predictions of the model. Does this mean that no appropriate solution can be found in this framework? In fact, the central difficulty for an optimal control approach to redundancy is to formulate the problem in such a way that it accounts for the simultaneous control of posture and movement. Most studies have not considered the case of static forces. Some studies that have actually tackled this problem have reported difficulties in solving optimal control problems in the presence of gravitational forces (Soechting and Flanders 1998; Thoroughman and Feller 2003). When a movement consists of a transition between two equilibrium postures, the boundary conditions of the optimal control problem should specify terminal equilibrium signals, e.g., muscle forces that compensate for applied static (elastic, gravitational) forces. The idea to add to the cost function a term that enforces given initial and final equilibrium postures (Dornay et al. 1996; Harris and Wolpert 1998) should lead to solutions that depend on the level and nature of the static forces. Although this issue has not been fully addressed in experimental studies, the results of Nishikawa et al. (1999) clearly suggest that dynamic and static controls are unlikely to be dealt with simultaneously. In contrast, the separation principle allows the application of optimal feedback control to kinematic redundancy problems with static forces because there is no a priori specification of the final posture of the limb.

An integral component of feedback control is the presence of a state estimator, i.e., a process that combines sensory inflow and motor outflow to provide an estimate of the current state of the system (Wolpert et al. 1995). A state estimator is necessary because *1)* the state is in general not directly observable and must be inferred from sensory inputs (e.g., vision, proprioception) and *2)* both inflow and outflow are noisy. It has been suggested that the nervous system acts as an optimal estimator (Baddeley et al. 2003; Wolpert et al. 1995). The optimal feedback control principle embeds an optimal estimator.

MAXIMUM EFFICIENCY PRINCIPLE. Optimal control is associated with the choice of a *cost function* (which indicates a quantity to minimize) and a *constraint function* (which specifies constrains to satisfy) (Nelson 1983). Here, we consider a cost function based on the size of centrally generated signals that eventually generate the dynamic forces. The reason for this choice is twofold. First, it is simple and easily measurable by the CNS, compared with other cost functions encountered in motor control literature that require complex calculations and measurement processes (acceleration derivative, torque change, energy, etc.). Second, related cost functions were successfully used in recent models (Harris and Wolpert 1998; Todorov and Jordan 2002). As a constraint function, we use the initial and final boundary conditions. The rationale for this choice, which differs from the mixed error/effort cost of Todorov and Jordan (2002), is the following. The error/effort cost function contains parameters that weight the respective contribution of state errors (position, velocity, force, etc.) and effort in the cost function. Because different sets of parameters lead to different behaviors, a model based on error/effort minimization cannot provide a univocal description of motor control. This problem has little consequence for the study of motor variability (Todorov and Jordan 2002), but is critical for the study of redundancy.

CONSTANT EFFORT PRINCIPLE. The idea of motor behavior being associated with the minimum of a cost function is appropriate when both movement amplitude and duration are specified. Otherwise, infinitely slow/fast or infinitely short/long movements could result. In cases where movement time is not given (e.g., instruction is to move at preferred speed), actual duration can be deduced by associating a desired level of effort with the instruction and using the relationship between amplitude, duration, and effort prescribed by the maximum efficiency principle. In this framework, the constant effort principle states that a given set of instructions is equivalent to a level of effort. For these instructions, movements of different amplitudes, directions, or against different loads are executed with the same effort.

A simple example

To illustrate the model, we consider the control of an inverted pendulum in the gravity field (Fig. 1*A*). The dynamics of the pendulum is given by

$$I_0(d^2\theta/dt^2) + m_0 g L_0 \cos \theta = u \qquad (1)$$

where θ defines the position of the pendulum; I_0, m_0, and L_0 are the inertia, mass, and length of the pendulum, respectively; and u is a control (here a torque). The control problem is to find $u(t)$ (t in $[t_0; t_f]$) such that $\theta(t_0) = \theta_0$ and $\theta(t_f) = \theta_f$ (Fig. 1*A*). According to the separation principle, we can write

$$u(t) = u_{dyn}(t) + u_{stat}(t)$$

where $u_{stat}(t)$ compensates for the effect of static forces (see *Eq. 3* below) and $u_{dyn}(t)$ is the solution to the control problem in the absence of static forces. To obtain $u_{dyn}(t)$, we apply the optimal feedback control principle and the maximum efficiency principle. At each time t_c, a control $u_{dyn}(t)$ is computed for the remaining duration (t in $[t_c; t_f]$) based on the planned displacement from the currently estimated position of the
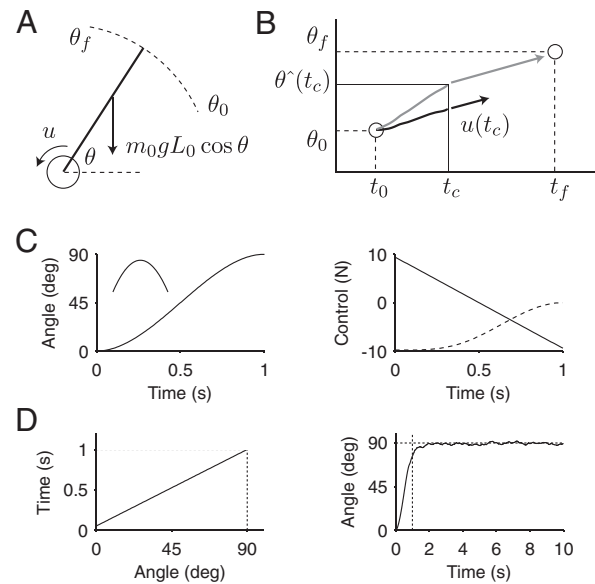

FIG. 1. *A*: inverted pendulum in the gravity field. *B*: in the presence of noise, the estimated trajectory of the pendulum (gray) deviates from its actual trajectory (black). At a given time t_c, the control $u(t_c)$ is calculated based on the estimated error (gray arrow) and is applied to the current state of the pendulum (black arrow). *C*: application of the model to a displacement between 0 and 90° in 1 s. *Left*: angle of the pendulum, velocity in *inset*. *Right*: dynamic (plain) and static (dashed) control. For simplicity, we used $I_0 = 1$, $m_0 = 1$, $L_0 = 1$. *D*: same as *C* in the presence of additive Gaussian noise ($\sigma = 0.4$). *Left*: amplitude/duration scaling. Dotted lines: 90° in 1 s. A nonzero intercept (here 0.05 s) was necessary for appropriate functioning of the controller. *Right*: angle of pendulum. Dotted lines: 1 s, 90°.

pendulum [$\theta^\wedge(t_c)$, which is generally different from $\theta(t_c)$ arising from noise or perturbation] to the target position θ_f (Fig. 1*B*). The control $u_{dyn}(t_c)$ is applied and the process starts again at the next time step. The mathematical solution to this problem is obtained using the Euler–Lagrange equation (e.g., Hogan 1984; Kirk 1970)

$$d^2[\partial u_{dyn}^2/\partial(d^2\theta/dt^2)]/dt^2 = 0 \qquad (2)$$

with boundary conditions $\theta(t_c) = \theta^\wedge(t_c)$ and $\theta(t_f) = \theta_f$. For this problem, we have

$$u_{stat}(t_c) = m_0 g L_0 \cos \theta^\wedge(t_c) \qquad (3)$$

which reflects the fact that the state of the pendulum is not known, but can only be estimated.

In the absence of noise and perturbations, we see that the control calculated at t_0 for the whole movement duration $[t_0; t_f]$ (open-loop control) is the same as the control recalculated at each time step (closed-loop control). An example of solution to *Eq. 2* in the absence of noise and perturbations is shown in Fig. 1*C*. An open question is whether the controller is stable in the presence of noise. We simulated the same example in the case where

$$\theta^\wedge(t) = \theta(t) + n(t)$$

where $n(t)$ is a zero-mean Gaussian noise with variance σ^2. Because of noise, the pendulum will in general never reach its target position. Thus movement duration could not be fixed in advance and was determined by an amplitude/duration law—i.e., at each time, the remaining duration was a function of the residual distance to the target (Fig. 1*D*, *left*). The pendulum

reached the vicinity of the target and then smoothly oscillated around it (Fig. 1*D*, *right*). This result was robustly observed over a broad range of parameters (variance of noise, slope of the amplitude/duration law). Thus stable control of a naturally unstable system can be obtained with the principles of the model in the linear case. Stability arises from the action of the dynamic controller, which attempts to reduce the distance between the estimated state of the pendulum and the target, but not of the static controller, which simply compensates for gravity.

General sketch of the model

The model is summarized in Fig. 2*A*. It has three components: *1*) a *dynamic controller*, which calculates, for given target (goal) and estimated states, the appropriate control to master the dynamic forces and progress toward the goal (dashed arrow on the *left*); *2*) a *static controller*, which calculates for each estimated state the appropriate control that maintains equilibrium against the static forces (dashed arrow on the *right*); *3*) a *state estimator*, which calculates a state estimate from sensory inflow and motor outflow (gray arrows).

Scope of the article

The four principles have been proposed to address Bernstein's problem. However, the present article concerns the part of the problem related only to kinematic redundancy. The goal of this article is to show that the dynamic controller can solve the problem of kinematic redundancy in a way that is consistent with experimental observations. Thus we focused on the dynamic controller and we used the following simplifications (Fig. 2*B*). First, because neither perturbations nor noise was introduced, no state estimator was needed and optimal feedback control was strictly equivalent to open-loop optimal control (see Fig. 1*B*). Thus simulations described below were obtained using a method to solve open-loop control problems. Second, the static controller was not modeled. We assumed that there were no static forces or, equivalently, that the static forces were exactly cancelled at each time step during the movement. The complete model including static and dynamic forces was not simulated.

METHODS

Modeling approach

The principles were cast in computational terms so they needed to be translated into simulations for comparisons with experimental

observations. A central issue was the representation of the neuromuscular system. In fact, it is a complex machinery that contains both intricate neural circuits and noisy nonlinear elements for action and sensation, so an open question is the degree of biological realism that can guarantee that a simulation is a useful reflection of biological operations. Although there is no general answer to this question, we addressed it using two principles: *1*) start with a simple model; if it does not work, then try a more complex one; and *2*) of two models that provide similar results, the simplest is the best.

According to the first principle, we built on simple hypotheses. At a basic level of details, we focused on four main properties of the muscle: *1*) it generates forces when it is stimulated; *2*) it behaves like a linear spring; *3*) it performs low-pass filtering; and *4*) it is inserted around a joint and generates a torque. We also assumed that *1*) a muscle is made of a single type of fibers that are all innervated by the same motoneuron; *2*) a motoneuron receives a unique and specific control signal (see *Controlled object*). Because linear springlike forces are static forces, they were removed according to the separation principle. The results obtained with these hypotheses were in adequate correspondence with experimental data. For comparisons, we built more complex models. A muscle is in fact a nonlinear spring so we included a force/velocity relationship. A muscle can act on several joints so we considered biarticular muscles. A muscle can be controlled through muscular synergies. We first describe the results obtained with the simplest model that best highlight the power of the proposed principles. Then we show results obtained with biarticular muscles (see *Muscular redundancy*), nonlinear muscles (see *Influence of muscle properties*), and muscular synergies (see *Muscular synergies*).

Controlled object

The controlled object was modeled as a rigid, multilink, articulated system with N DOF. It was actuated by one pair of antagonist muscles per DOF. Each muscle i ($1 \leq i \leq 2N$) was controlled by a motoneuron and the ensemble motoneuron + muscle (neuromuscular system) was modeled as a second-order low-pass filter (van der Helm and Rozendaal 2000), which transforms a *neural control signal* (u_i) into a muscular force (F_i) according to

$$\nu(de_i/dt) = -e_i + u_i$$
$$\nu(da_i/dt) = -a_i + e_i \qquad (4)$$
$$F_i = \eta(a_i)$$

where ν is a time constant and $\eta(z) = [z]^+$ ($[z]^+ = z$ if $z > 0$; otherwise, $[z]^+ = 0$). This latter function was used to express the fact that a muscle exerts only a pulling force. The terms for these quantities e_i and a_i correspond to excitation and activation, respectively. Electromyographic (EMG) activity was defined as $[e_i]^+$. Torques were calculated at each DOF as the difference between the forces generated by antagonist muscles scaled by a coefficient (γ; see following text).

The dynamics of the controlled object and the neuromuscular system was described by

$$d\mathbf{x}/dt = f[\mathbf{x}(t), \mathbf{u}(t)] \qquad (5)$$

where $\mathbf{x}$ describes the state of the object (angular position and velocity) and the muscles (activation, excitation). *Equation 5* contained *Eq. 4* for each muscle and the equations for movement dynamics (see *Kinematic chains*).

Optimal controller

Point-to-point trajectories of the controlled object were obtained as solutions of an optimal control problem: find deterministic controls $\mathbf{u}(t) = \{u_i(t)\}$ ($1 \leq i \leq 2N$) in $[t_0; t_f]$ such that $\mathbf{x}(t)$ is a solution to *Eq. 5* with boundary conditions
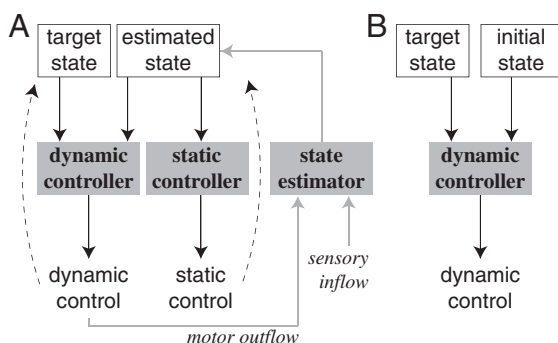

FIG. 2.   *A*: general sketch of the model. *B*: focus of the present article.

$$\mathbf{x}(t_0) = \mathbf{x_0} \quad \text{and} \quad \psi[\mathbf{x}(t_f)] = 0 \qquad (6)$$

and the quantity

$$E^2 = \sum_{i=1\cdots 2N} \int_{[t_0;t_f]} u_i^2(t) dt \qquad (7)$$

is minimum (we use the generic term *effort* for the quantity E; Todorov and Jordan 2002). Function ψ expresses constraints on the final state of the system (see following text). Any kind of constraint can be handled. For instance, ψ was $\mathbf{x}(t_f) - \mathbf{x_f}$ for nonredundant objects ($\mathbf{x_f}$ is the desired final boundary value).

Constant effort principle

The optimal control model can be used to calculate control signals that drive the arm from an initial position to a target position (movement of amplitude A) in a given time (duration $D = t_f - t_0$). By construction, the control signals are unique and their associated effort is E (*Eq. 7*). We can repeat this operation for different amplitudes and different durations and build a surface $E = E(A, D)$. This relationship is monotonic because it increases with A and decreases with D (larger or faster movements require larger controls). Conversely, if A and $E = E_c$ are given, it defines a unique duration D. The relationship between movement amplitude and duration corresponding to a given effort (E_c) was obtained by building the surface $E = E(A, D)$ and searching the intersection between this surface and the plane $E = E_c$. The surface was obtained by interpolation between calculated points on a grid.

Kinematic chains

We considered several kinematic chains that illustrate different aspects of redundancy (Fig. 3). A kinematically nonredundant system was used to study kinematic invariance and muscular redundancy (Fig. 3*C*). A chain is specified by a set of joint angles (q_i, $i = 1\ldots N$)
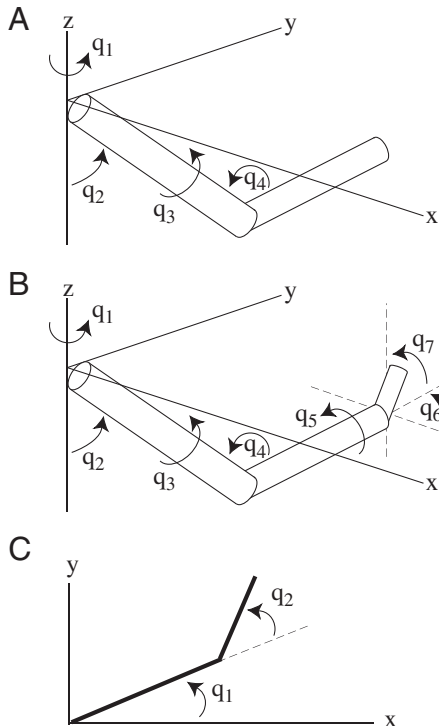

FIG. 3. Kinematic chains. *A*: 4 degrees of freedom (4-DOF), 2-link chain in 3-dimensional (3D) space. *B*: 7-DOF, 3-link chain in 3D space. *C*: 2-DOF, 2-link chain in 2D space.

that define a kinematic transformation (from angular to Cartesian coordinates). The equations for movement dynamics were derived using the Euler-Lagrange method (Spong and Vidyasagar 1989). Briefly, four steps were necessary: *1*) the rotation vector of each segment was calculated; *2*) translational and rotational kinetic energies were calculated; *3*) the Lagrangian L was obtained as the sum of kinetic energies; and *4*) torques T_i at each DOF were calculated using

$$T_i = d[dL/d(dq_i/dt)]/dt - dL/dq_i$$

which leads to

$$T_i = \sum_{j=1\cdots N} A_{ij}(d^2q_j/dt^2) + C_i \qquad (8)$$

Coefficients A_{ij} and C_i were obtained with a tool for symbolic calculus. *Equation 8* was then inverted to obtain relationships between angular accelerations and torques, which were inserted into *Eq. 5*. For illustration, the resulting equations are given below for $N = 2$. The other cases involve lengthy equations that cannot be reproduced here (e.g., for $N = 7$, *Eq. 8* requires more than 200,000 elementary operations $[+, -, \times, \cos, \sin]$).

4-DOF, 2-LINK CHAIN IN 3D SPACE (FIG. 3A). In this case, $N = 4$. The effector had two segments (upper arm, forearm) and two joints (shoulder, elbow) with 3 DOF at the shoulder and 1 DOF at the elbow. Arm kinematics was represented by

$$r_1 = L_1 \sin(q_1)\sin(q_2) + L_2\{[(\cos(q_1)\cos(q_3)$$
$$- \sin(q_1)\cos(q_2)\sin(q_3)]\sin(q_4) + \sin(q_1)\sin(q_2)\cos(q_4)\}$$

$$r_2 = -L_1\cos(q_1)\sin(q_2) + L_2\{[(\sin(q_1)\cos(q_3)$$
$$+ \cos(q_1)\cos(q_2)\sin(q_3)]\sin(q_4) - \cos(q_1)\sin(q_2)\cos(q_4)\}$$

$$r_3 = L_1\cos(q_2) + L_2[\sin(q_2)\sin(q_3)\sin(q_4) + \cos(q_2)\cos(q_4)]$$

where (r_1, r_2, r_3) are the endpoint coordinates; (q_1, q_2, q_3, q_4) are the shoulder azimuth angle, the shoulder elevation angle, the shoulder intrinsic (humeral) rotation angle, and the elbow rotation angle, respectively; and L_1, L_2 are the upper arm and forearm lengths. As a result of redundancy, final arm configuration was specified indirectly by the desired endpoint coordinates in function ψ (*Eq. 6*). Initial arm configuration was (q_1, q_2, q_3, q_4) = (120, 140, 30, 90°).

7-DOF, 3-LINK CHAIN IN 3D SPACE (FIG. 3B). In this case, $N = 7$. The effector had three segments (upper arm, forearm, hand) and three joints (shoulder, elbow, wrist) with 3 DOF at the shoulder, 2 DOF at the elbow, and 2 DOF at the wrist. Arm kinematics was represented by

$$r_1 = \langle(([\cos(q_1)\cos(q_3) - \sin(q_1)\cos(q_2)\sin(q_3)]$$
$$\times [-\cos(q_5)\sin(q_7) - \sin(q_5)\cos(q_6)\cos(q_7)]L_3$$
$$+ [-\cos(q_1)\sin(q_3) - \sin(q_1)\cos(q_2)\cos(q_3)]$$
$$\times \{[-\cos(q_4)\sin(q_5)\sin(q_7)] + [\cos(q_4)\cos(q_5)\cos(q_6)$$
$$- \sin(q_4)\sin(q_6)]\cos(q_7)\}L_3 - \sin(q_4)L_2\rangle$$
$$+ \sin(q_1)\sin(q_2) \times \{[-\sin(q_4)\sin(q_5)\sin(q_7)$$
$$+ [\sin(q_4)\cos(q_5)\cos(q_6) + \cos(q_4)\sin(q_6)]\cos(q_7)\}L_3$$
$$+ \cos(q_4)L_2 + L_1)$$

$$r_2 = (\langle[\sin(q_1)\cos(q_3) + \cos(q_1)\cos(q_2)\sin(q_3)]$$
$$\times [-\cos(q_5)\sin(q_7) - \sin(q_5)\cos(q_6)\cos(q_7)]L_3$$
$$+ [-\sin(q_1)\sin(q_3) + \cos(q_1)\cos(q_2)\cos(q_3)]$$
$$\times \{[-\cos(q_4)\sin(q_5)\sin(q_7) + [\cos(q_4)\cos(q_5)\cos(q_6)$$
$$- \sin(q_4)\sin(q_6)]\cos(q_7)\}L_3 - \sin(q_4)L_2\rangle$$

$$- \cos(q_1) \sin(q_2) \times \{[-\sin(q_4) \sin(q_5) \sin(q_7)$$
$$+ [\sin(q_4) \cos(q_5) \cos(q_6) + \cos(q_4) \sin(q_6)] \cos(q_7)\}L_3$$
$$+ \cos(q_4)L_2 + L_1\rangle$$

$$r_3 = \sin(q_2) \sin(q_3)[-\cos(q_5) \sin(q_7) - \sin(q_5) \cos(q_6) \cos(q_7)]L_3$$
$$+ \sin(q_2) \cos(q_3)\langle\{[-\cos(q_4) \sin(q_5) \sin(q_7)$$
$$+ [\cos(q_4) \cos(q_5) \cos(q_6) - \sin(q_4) \sin(q_6)]L_3$$
$$- \sin(q_4)L_2\rangle + \cos(q_2)\{[-\sin(q_4) \sin(q_5) \sin(q_7)]$$
$$+ [\sin(q_4) \cos(q_5) \cos(q_6) + \cos(q_4) \sin(q_6)]L_3 + \cos(q_4)L_2 + L_1\rangle$$

where (r_1, r_2, r_3) are the endpoint coordinates; $(q_1, q_2, q_3, q_4, q_5, q_6, q_7)$ are the shoulder azimuth angle, the shoulder elevation angle, the shoulder intrinsic (humeral) rotation angle, the elbow rotation angle, the elbow intrinsic rotation angle, the wrist flexion/extension angle, and the wrist pronation/supination angle, respectively; and L_1, L_2, L_3 are the upper-arm, forearm, and wrist lengths. Initial arm configuration was $(q_1, q_2, q_3, q_4, q_5, q_6, q_7) = (120, 120, 90, 90, 60, 90, 10°)$. As a result of redundancy, final arm configuration was specified indirectly by the desired endpoint coordinates and desired hand orientation in function ψ (*Eq. 6*). In fact, the target was an elongated object and the constraints were that *1*) the endpoint of the arm matches the center of gravity of the object and *2*) the hand (i.e., the vector in the plane of the hand and perpendicular to its long axis) is oriented parallel to the long axis of the object.

2-DOF, 2-LINK CHAIN IN 2D SPACE (FIG. 3C). In this case, $N = 2$. The controlled system had two segments (upper arm, forearm) and two joints (shoulder, elbow) with 1 DOF per segment. Kinematics was represented by

$$r_1 = L_1 \cos(q_1) + L_2 \cos(q_1 + q_2)$$
$$r_2 = L_1 \sin(q_1) + L_2 \sin(q_1 + q_2)$$

where (r_1, r_2) are the endpoint coordinates; (q_1, q_2) represent the shoulder and elbow angles, respectively; and L_1, L_2 are the upper arm and forearm lengths. In general, initial arm configuration was $(q_{10}, q_{20}) = (45, 90°)$. Desired final configuration was (q_{1f}, q_{2f}). The state vector was expressed by

$$\mathbf{x}(t) = [q_1(t), q_2(t), v_1(t), v_2(t), a_1(t), a_2(t), a_3(t), a_4(t), e_1(t), e_2(t), e_3(t), e_4(t)]$$

where $v_1(t) = dq_1/dt$ and $v_2(t) = dq_2/dt$ (angular velocities). The dynamics of the arm + muscles was expressed by the following series of equations

$$dv_1(t)/dt = [(T_{sh} - C_1)A_{22} - (T_{ei} - C_2)A_{12}]/(A_{11}A_{22} - A_{12}A_{21})$$
$$dv_2(t)/dt = [(T_{el} - C_2)A_{11} - (T_{sh} - C_1)A_{21}]/(A_{11}A_{22} - A_{12}A_{21})$$
$$v(da_i/dt) = -a_i + e_i \quad (i = 1, 2, 3, 4)$$
$$v(de_i/dt) = -e_i + u_i \quad (i = 1, 2, 3, 4)$$

where

$$T_{sh} = \gamma_{sh}[\eta(a_1) - \eta(a_2)] \quad \text{and} \quad T_{el} = \gamma_{el}[\eta(a_3) - \eta(a_4)] \qquad (9)$$

are muscular shoulder and elbow torques, respectively, and

$$A_{11} = I_1 + I_2 + m_1 L_{c1}^2 + m_2[L_1^2 + L_{c2}^2 + 2L_1 L_{c2} \cos(q_2)]$$
$$A_{12} = I_2 + m_2[L_{c2}^2 + L_1 L_{c2} \cos(q_2)]$$
$$C_1 = -m_2 L_1 L_{c2} v_2^2 \sin(q_2) - 2m_2 L_1 L_{c2} v_1 v_2 \sin(q_2)$$
$$A_{21} = A_{12}$$
$$A_{22} = I_2 + m_2 L_{c2}^2$$

$$C_2 = m_2 L_1 L_{c2} v_1^2 \sin(q_2)$$

with $L_{c1} = c_1 L_1$ and $L_{c2} = c_2 L_2$ (distance from rotation axis to the center of gravity of the segments), and where m_1, m_2 represent the mass of the segments, and I_1, I_2 are the moments of inertia of the segments. The boundary conditions were

$$\mathbf{x_0} = [q_{10}, q_{20}, 0, 0, 0, 0, 0, 0, 0, 0, 0, 0]$$

and

$$\mathbf{x_f} = [q_{1f}, q_{2f}, 0, 0, 0, 0, 0, 0, 0, 0, 0, 0]$$

(Velocities and forces were zero at the beginning and end of the movement.) More generally, any boundary conditions can be used (nonzero velocities or forces).

Numerical methods

The problem defined by *Eqs. 5*, *6*, and *7* is an optimization problem that can be transformed into a differential equation problem using the calculus of variations (Kirk 1970). The differential equation problem is a two-point boundary-value problem, i.e., a differential system with boundary conditions at initial and final times. Solutions to this problem were obtained numerically using a gradient method (Bryson 1999). Function $\eta(z) = [z]^+$ is not differentiable and was replaced by the differentiable function $z \to \log[1.0 + \exp(\kappa z)]/\kappa$.

Parameters

General parameters were $\nu = 0.04$ s (time constant of muscle filtering) and $\kappa = 10$ (characteristic of muscle force generation). Other parameters were specific to each kinematic chain. Each segment i (1: upper arm; 2: forearm; 3: hand) is defined by a mass (m_i in kilograms), a length (L_i in meters), a center of gravity (c_i in percentage of the length), and moments of inertia along and perpendicular to its main axis (J_i and I_i in kilograms per square meter). For each DOF, there is a coefficient γ (in meters) that translates force into torque.

For $N = 2$, parameters were $m_1 = 2.52$, $L_1 = 0.33$, $c_1 = 0.5$, $I_1 = 0.023$, $m_2 = 1.3$, $L_2 = 0.4$, $c_2 = 0.5$, $I_2 = 0.011$, and $\gamma_{sh} = \gamma_{el} = 0.04$. The choice of γ_{sh} and γ_{el} is somewhat arbitrary. In fact, these parameters result from the interplay between: *1*) the innervation ratio of the muscles acting at shoulder and elbow; *2*) the moment arm of these muscles; and *3*) the modulation of force production by firing rate and recruitment in pools of motoneurons. Rather than doing a complex estimation based on the contribution of these factors, we explored the influence of γ_{sh} and γ_{el} on the behavior of the model. The model was mostly insensitive to the values of γ_{sh} and γ_{el} as long as the ratio γ_{el}/γ_{sh} was neither too small (>0.05) nor too large (<1.2).

For $N = 4$, parameters were as defined for $N = 2$ and $J_1 = 0.0013$, $\gamma_1 = 10$, $\gamma_2 = 10$, $\gamma_3 = 10$, and $\gamma_4 = 5$.

For $N = 7$, parameters were as defined for $N = 4$, but $m_2 = 1.3$, $L_2 = 0.25$, $I_2 = 0.0074$ (shorter forearm), and $m_3 = 0.49$, $L_3 = 0.15$, $c_3 = 0.25$, $I_3 = 0.001$, $J_3 = 0.0005$, $\gamma_5 = 1$, $\gamma_6 = 1$, and $\gamma_7 = 1$.

When a mass m_a was added to a segment (length L, inertia I, mass m, center of mass c) at position L_a, the new inertia of the segment was

$$I + mc^2 + m_a L_a^2 - m_a(mc + m_a L_a)^2/(m + m_a)^2 \qquad (10)$$

Comparison with experimental data

The model is a parameter-free model, i.e., all the parameters are well defined and constant for a given individual at a given time (e.g., forearm inertia). As a consequence, we did not try to provide the best fits to the experimental data because *1*) fitting is general associated with arbitrary parameter adjustments and *2*) fitting quality may not be sufficient to estimate the validity of a model (e.g., see the debate between minimum-jerk and minimum torque change models of motor control; Flash 1990). The results reported here are meant to demon-

strate the power of the concepts underlying the model, rather than account for a few selected aspects of the behavior. When possible, we indicate in the text a reference to one or more published figures that can be used for comparisons with the model.

RESULTS

We describe implications of the proposed principles for point-to-point movements. Except for cases dealing with kinematic redundancy, the 2-DOF arm was used. Except for cases illustrating the constant effort principle, the simulated movements were specified by their amplitude and duration.

Kinematic redundancy

3D POINTING MOVEMENTS. We simulated optimal point-to-point trajectories of a 4-DOF arm in 3D space (Fig. 3A). An example is illustrated in Fig. 4A for a forward/upward/leftward movement. The trajectory was curved, planar, independent of speed, and the tangential velocity had a bell-shaped profile (Fig. 4A). Further examples of trajectories and velocity profiles are shown for movements in a frontal (Fig. 4, B and C) and sagittal (Fig. 4, D and E) plane (for comparison, see Fig. 3 in Flanders et al. 1996; Fig. 1 in Gottlieb et al. 1997). Hand path curvature varied with movement direction and went through one cycle (Fig. 4F). We note that quantitative data on movement curvature are scarce. The most complete study is for vertical movements in a sagittal plane (Flanders et al. 1996; Pellegrini and Flanders 1996). Curvature could be described by: curvature = cos (direction + phase), which also holds for the model (for comparison, see Fig. 2 in Pellegrini and Flanders 1996). However, we cannot expect to obtain an exact fit because the phase should depend on arm posture and the hypothesized mechanical actions of the muscles (in the data of Pellegrini and Flanders 1996, the phase varied across subjects). Soechting and Flanders (1998) showed that neither minimum-torque change nor minimum-muscle force change models can explain the pattern of curvature for vertical movements. The terminal posture was independent of movement velocity (Fig. 4, G and H). These observations were qualitatively similar for all tested movements and were consistent with experimental observations (Alexandrov et al. 1998; Atkeson and Hollerbach 1985; Flanders et al. 1999; Hermens and Gielen 2004; Klein Breteler et al. 1998; Nishikawa et al. 1999; Pellegrini and Flanders 1996; Soechting and Lacquaniti 1981; Torres and Zipser 2004; Zhang and Chaffin 1999). The terminal posture was also independent of forearm inertia (<2 deg of variations for movements in Fig. 4, B and D) over the tested range (using a weight of 0.6–1.6 kg attached to the forearm at $3L_2/4$ from the elbow; Hermens and Gielen 2004). We verified that the terminal posture depended on initial posture (Gielen et al. 1997; Hermens and Gielen 2004; Soechting et al. 1995). However, a quantitative study was not pursued on this point because these studies did not report actual initial postures of the arm that were used. Initial hand positions are not sufficient in this case. A quantitative analysis would require establishing the relationship between initial and final arm angles across a large range of movements (different initial postures, different directions). This issue was addressed in the context of grasping movements (see following text; Fig. 7).

According to the separation principle, trajectories should not be influenced by gravity, which is at variance with experimen-
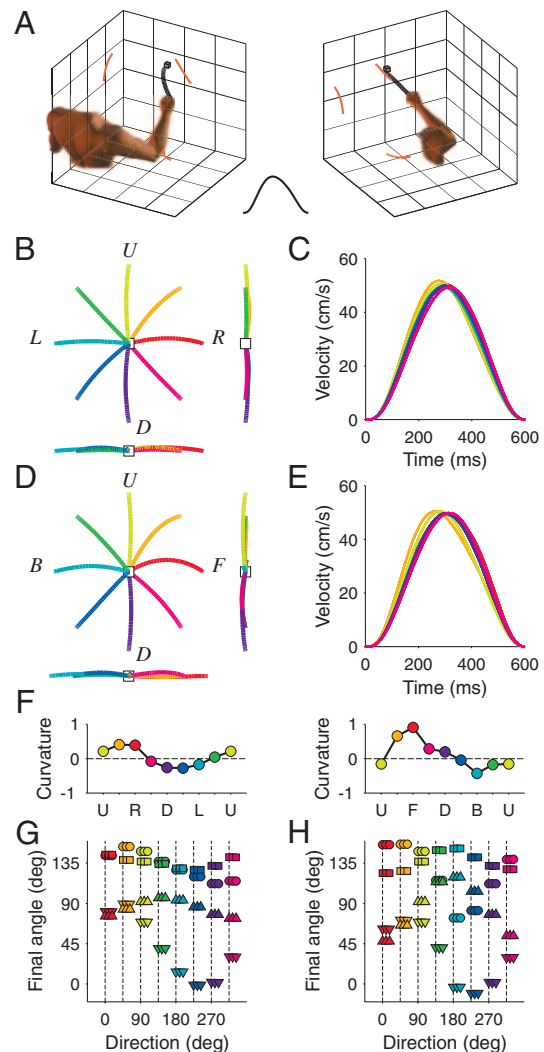

FIG. 4. Optimal control for a redundant arm. A: 2 views of a simulated trajectory for a forward/leftward/upward movement (20 cm, 600 ms). Inset: tangential velocity profile. B: movements in 8 directions (15 cm, 600 ms) in the frontal plane projected on this plane (left), on a sagittal plane (right), and on a dorsal plane (bottom). U, up; F, forward; D, down; B, backward. C: tangential velocity profiles for the movements in B. D: movements in 8 directions in a sagittal plane projected on this plane (left), on a frontal plane (right), and on a dorsal plane (bottom). R, right; L, left. E: tangential velocity profiles for the movements in D. F: hand path curvature (in millimeters) measured as the mean deviation from straight line (counterclockwise deviation >0) for data in B (left) and D (right). G: final angular positions (circle: q_1; box: q_2; down triangle: q_3; up triangle: q_4) for the movements in B at 3 velocities (600, 800, 1,000 ms). Offsets have been used to reveal superimposed points. H: same as G for data in D.

tal observations (Atkeson and Hollerbach 1985; Papaxanthis et al. 2003). However, results on up–down and down–up movements are ambiguous because movement trajectories may depend not only on gravity, but also on initial and terminal positions. Thus direction-dependent hand paths can be expected in an optimal control model in the absence of gravity. This was found in the model (Fig. 5). In particular, we observed differences between upward and downward trajectories (Fig. 5A) and between the corresponding velocity profiles (Fig. 5B) (for a comparison, see Fig. 2 in Papaxanthis et al. 2003). These results indicate that the observed differences between upward and downward movements are not incompat-
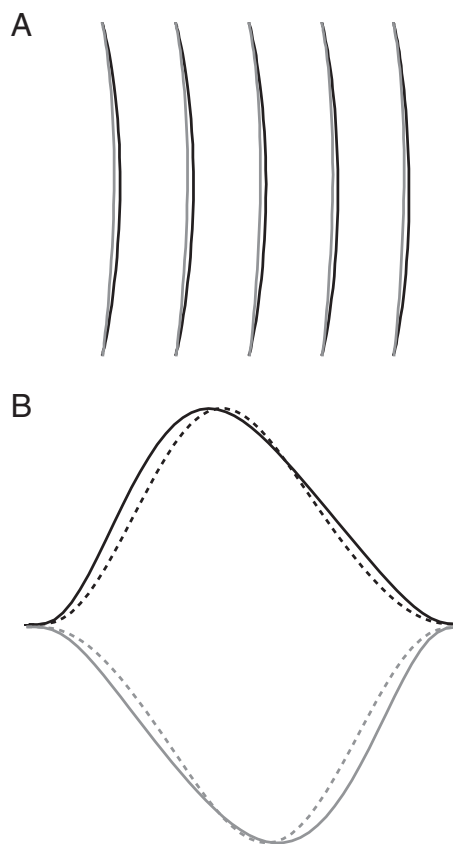
A

B

FIG. 5. Upward/downward movements. Simulation of the 4-DOF arm (same model as in Fig. 4) for 400- to 1,200-ms, 30-cm upward and downward movements. Initial posture for upward movement was as in Fig. 4. Initial posture for downward movements was the final posture of upward movements. *A*: trajectories (black: upward; gray: downward) projected on a frontal plane (as viewed when facing the subject). *B*: normalized velocity profiles for upward (black) and downward (gray) movements (solid: 600 ms; dashed: 400 ms).

ible with the separation principle. More behavioral data, including systematic variations of movement kinematics with initial and final position, would be necessary to distinguish between gravity and position effects.

Grasping movements

An additional source of redundancy arises for the control of a distal segment, such as a hand that grasps an object. Additional degrees of freedom are related to hand orientation and aperture and additional constraints are provided by the shape of the object. We addressed the control of hand orientation with a 7-DOF arm (Fig. 3*B*). We simulated movements toward an elongated object at different locations (see METHODS).

The trajectories were similar to those observed with a 4-DOF arm (Fig. 6*A*). The model exhibited coarticulation of hand transport and rotation along the path (Fig. 6*B*). There was a linear relationship between movement direction and hand azimuth (Fig. 6*C*). These results are consistent with experimental observations (Bennis and Roby-Brami 2002; Cuijpers et al. 2004; Desmurget et al. 1996; Roby-Brami et al. 2000; Torres and Zipser 2004).

To assess how final posture depends on initial posture, we reproduced the experiment of Desmurget et al. (1998). Move-

ments from two initial postures (*high* and *low*) toward three targets (*sagittal*, *close*, *lateral*) were simulated. Final shoulder and elbow angles were generally different for movements toward the same target, but starting from different postures (Fig. 7). The variations were quantitatively similar to those observed experimentally (see Fig. 2 in Desmurget et al. 1998). A difference was found with respect to the variations of forearm rotation angle that could be explained by differences in initial hand orientation. This result was not self-evident a priori. Indeed, not all optimal control models are able to explain the effects of initial posture on final posture (Admiraal et al. 2004).
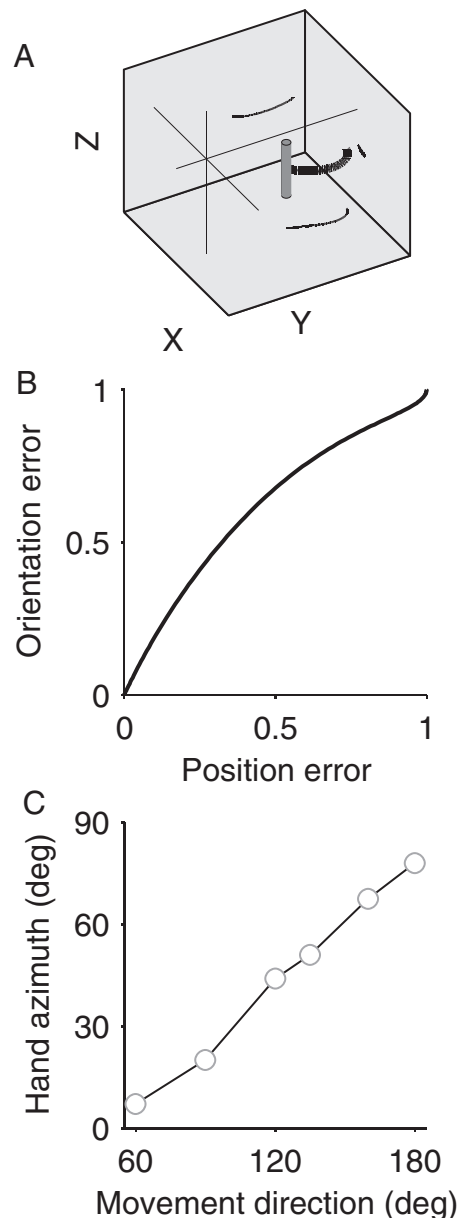
A

B

C

FIG. 6. Grasping movements with a 7-DOF arm. *A*: sample trajectory and velocity profile for a 20-cm, 600-ms movement (270 deg = toward the body). Target is indicated by a vertical cylinder. *B*: normalized time course of orientation error vs. time course of target distance error along the movement (coarticulation) for the movement in *A*. *C*: variations of hand azimuth with hand-centered movement direction (20-cm, 600-ms movements in the horizontal plane toward a vertical cylinder; movement direction is 0 deg rightward).
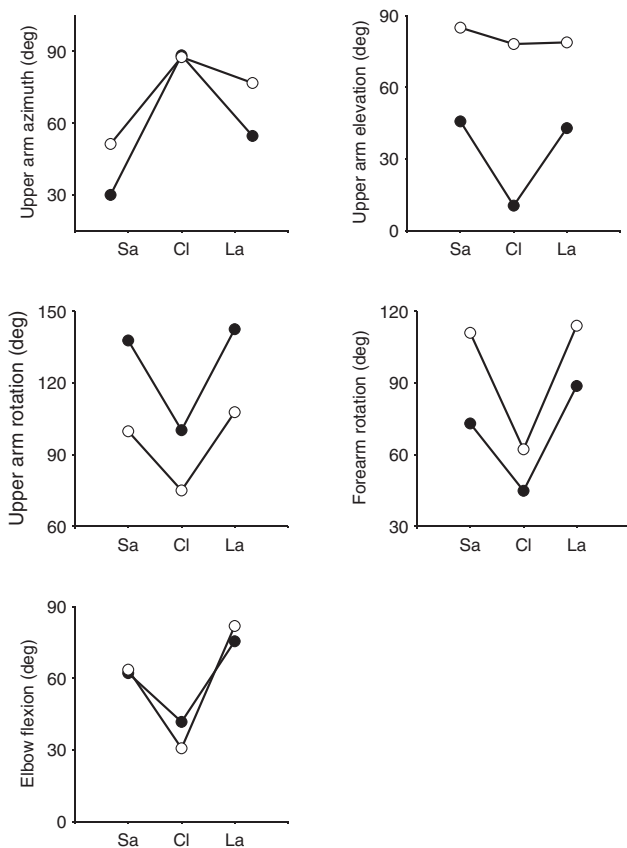
FIG. 7. Variations of final posture as the function of movement starting point (high, open circle; down, closed circle) and object position (Sa, sagittal; Cl, close; La, lateral) for a 7-DOF arm. Initial posture was (100, 105, 115, 80, 60, 90, 10) for high and (80, 160, 60, 80, 60, 90, 10) for down. Movement amplitude (in centimeters) and final hand orientation (two angles, in deg) were 53.5, 105.4, 74.2 (down→Sa), 52, −29.3, 82.2 (down→Cl), 55.8, 41.1, 67.4 (down→La), 31.3, 176.9, −11.1 (high→Sa), 26.7, −142.4, −13.0 (high→Cl), 12.3, 171.3, −29.3 (high→La). Movement duration was 600 ms.

Kinematic invariance

The proposed principles also have consequences that are not directly related to redundancy. These consequences were explored for a 2-DOF arm (Fig. 3C). When subjects perform movements of different amplitudes or against different inertial loads, they tend to use a single velocity profile that is scaled in time and amplitude (Atkeson and Hollerbach 1985; Bock 1990; Gordon et al. 1994; Kaminski and Gentile 1989). Invariant velocity profiles were observed as a consequence of the constant effort principle, i.e., for movements of different amplitudes when movement time was chosen to obtain a given effort level (Fig. 8A; for comparison see Fig. 3 in Gordon et al. 1994). In fact, the assumption that all movements are executed with the same effort leads to an implicit relationship between amplitude and duration, illustrated in Fig. 8B. For the eight directions tested, movement duration and peak velocity were linearly related to amplitude (Fig. 8, C and D; for comparison, see Fig. 4 in Gordon et al. 1994). The separation principle predicts that amplitude/duration scaling should be similar for upward and downward movements, previously observed experimentally (Virji-Babul et al. 1994). Moreover, movement duration and peak velocity varied with movement direction. As observed experimentally (Gordon et al. 1994; Turner et al. 1995), the duration was longer and peak velocity smaller for

directions parallel to the forearm (Fig. 8, E and F) in which the inertial load to be moved was larger (for comparison, see Fig. 6 in Gordon et al. 1994; Fig. 9 in Sober and Sabes 2003; see also Pellegrini and Flanders 1996, Fig. 3 and for vertical movements, Fig. 5 in Murata and Iwase 2001; see also Fernandez and Bootsma 2004; Jagacinski and Monk 1985; Smyrnis et al. 2000). The shape of velocity profiles was described by the ratio c between peak and average velocity (Ostry et al. 1987). This factor varied with the level of effort (Fig. 8G, inset), but was almost constant across amplitudes (Fig. 8G). Exceptions were observed in directions of larger curvature (Fig. 8, E and G). We tested the hypothesis that kinematic invariance is actually related to movement curvature. We simulated straight movements in the 135° direction by forcing the curvature to be as small as possible. We determined the amplitude/duration relationship and found that it was still linear and the velocity profile was strictly invariant. It should be noted that, in fact, kinematic invariance is an emergent
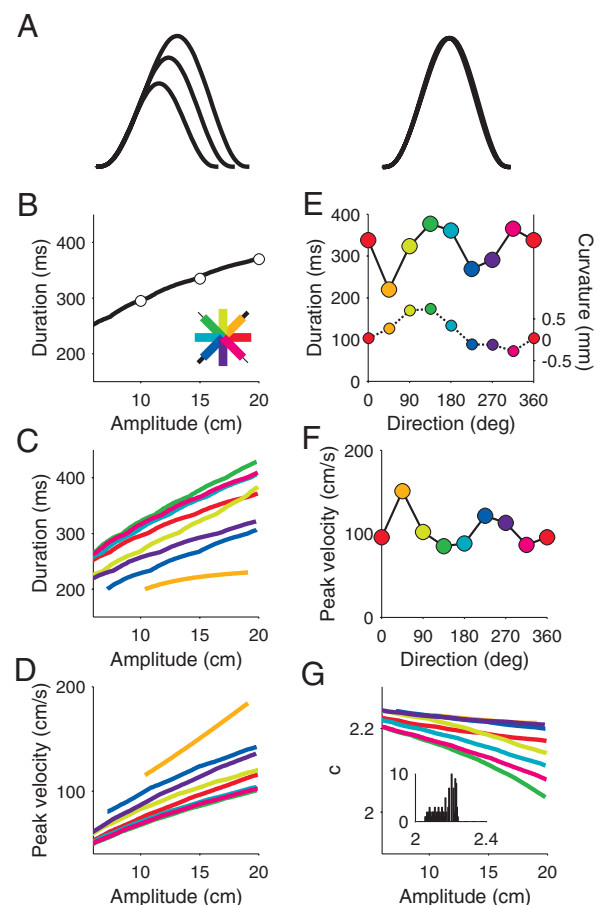

FIG. 8. A: kinematic invariance under constant effort ($E^2 = 10$) for a planar arm. Actual (left) and normalized (right) velocity profiles for 10, 15, and 20 cm rightward movements. B: movement duration vs. amplitude for rightward movements (circles correspond to profiles in A). Inset: correspondence between colors and directions; thick (thin) black line: minimum (maximum) inertia. 0° is rightward. C: movement duration vs. amplitude for 8 directions. D: peak velocity vs. amplitude. E: plain line: duration vs. direction for a given amplitude (15 cm). Dotted line: curvature vs. direction. Curvature was measured as the mean deviation (in millimeters) from straight line (positive for counterclockwise deviation). F: peak velocity vs. direction for a given amplitude (15 cm). G: $c = v_{peak}/v_{avg}$ vs. amplitude. Inset: distribution of c for 100 movements (5–20 cm, 200–500 ms, direction 0°). See METHODS for construction of this figure.
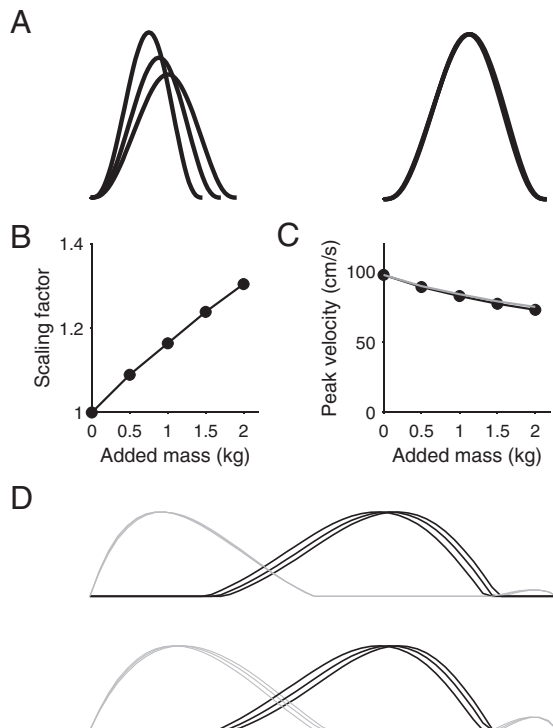
FIG. 9. *A*: kinematic invariance for added mass under constant effort ($E^2 = 10$) for a planar arm. Actual (*left*) and normalized (*right*) velocity profiles for a 15-cm rightward movement with 0, 1, and 2 kg added mass (m). Mass was a punctual mass at the arm endpoint. *B*: scaling factor in time: $k(m) = MT(m)/MT(m = 0)$, where MT is movement time. *C*: peak velocity vs. added mass (black line). Relation predicted by $v_{peak}(m) = v_{peak}(m = 0)/k(m)$ (gray line). *D*, *top*: normalized shoulder EMG for the 3 movements in *A* (flexor: black; extensor: gray). *Bottom*: normalized elbow EMG for the 3 movements in *A*.

property, given that no desired trajectory or velocity profile was specified for the simulated movements.

Constant effort also predicts invariance for inertial loads (Fig. 9*A*). These results were obtained by *1*) adding a mass at the arm endpoint and *2*) calculating optimal control solution for the system arm + mass (new inertia was calculated with *Eq. 10*). In this case, larger loads lead to slower movements. Interestingly, the timescaling factor (Fig. 9*B*) was very close to the amplitude-scaling factor (Fig. 9*C*) as observed experimentally (Figs. 2, 3, and 4 in Bock 1990; see also Hatzitaki and McKinley 2001). We note that scaling in time and amplitude occurred in the model in the absence of scaling at the level of joint torques, EMGs (Fig. 9*D*), and control signals (Gentner 1987; Zelaznik et al. 1986).

Muscular redundancy

Motor control systems master not only kinematic redundancy, but also muscular redundancy, e.g., because of the presence of biarticular muscles. An open question is how muscular redundancy would affect the preceding results obtained with a minimal agonist/antagonist organization. We first note that optimal control can actually tackle muscular redundancy (e.g., Dornay et al. 1996). Two biarticular muscles were introduced in the 2-DOF model: a shoulder/ elbow flexor and a shoulder/elbow extensor. Joint torques were (see *Eq. 9*)

$$T_{sh} = \gamma_{sh}[h(a_1) - h(a_2) + \alpha h(a_5) - \alpha h(a_6)]$$

$$T_{el} = \gamma_{el}[h(a_3) - h(a_4) + \alpha h(a_5) - \alpha h(a_6)]$$

where a_5 and a_6 are excitations for the biarticular flexor and extensor, respectively, and the α parameter specifies the contribution of the biarticular muscles relative to the monoarticular muscles. We chose $\alpha = 1$. On the one hand, the presence of biarticular muscles had little influence on movement kinematics (Fig. 10, *A* and *B*). On the other hand, the contribution of monoarticular shoulder and elbow muscles was dramatically modified (Fig. 10, *C* and *D*). Part of their original contribution was now subserved by the biarticular muscles (Fig. 10*E*). These observations were graded with respect to α. These results indicate that the covariations reported in preceding sections should be qualitatively immune to the presence of muscular redundancy. This does not mean that biarticular muscles are useless. In fact, from the perspective of a controller, mono- and biarticular muscles are not different—that is, they are exploited at best to satisfy the required constraints.

Influence of muscle properties

The preceding results were obtained using muscles modeled as force-generating elements. We assessed the influence of the force/length and force/velocity (called viscosity for simplicity) relationship in muscles (Hill model). Briefly, the force F generated by a muscle (*Eq. 4*) was used to calculate the maximal isometric force

$$F^{iso} = [1 + K(\lambda - \lambda_0)]F$$

where λ is muscle length and K is a parameter. The actual velocity-modulated muscle force was

$$F^{vel} = [bF^{iso} + a(d\lambda/dt)]/[b - (d\lambda/dt)] \quad \text{if } d\lambda/dt < 0 \text{ (shortening muscle)}$$

$$F^{vel} = [b'F^{iso} - (a' + 2F^{iso})d\lambda/dt]/[b' - (d\lambda/dt)]$$

$$\text{if } d\lambda/dt > 0 \text{ (lengthening muscle)}$$

where $d\lambda/dt$ is muscle velocity, $a' = -0.4F^{iso}$, $b' = -b(a' + F^{iso})/(a + F^{iso})$, $a = 250$, $b = 0.5$, $K = 0.1$ (Fig. 11*D*, *inset*). For simplicity, we assumed that muscle length was proportional to joint angle. As shown in Fig. 11, viscosity had a dramatic effect on EMGs (Fig. 11, *C* and *D*), but little influence on movement kinematics (Fig. 11, *A* and *B*). This result was confirmed over a broad range of movements. We did not find any remarkable properties related specifically to the presence of viscosity, i.e., properties that would be absent in the absence of viscosity. In fact, optimal control builds an internal model of the neuromuscular system. The muscular properties are exploited by the controller to reach its goal (for related ideas, see Todorov 2000). For instance, if a muscle generates less force because it is shortening, the controller could increase the control (change in EMG) or, if it is too costly, use another DOF (change in kinematics).

Muscular synergies

We assumed that *1*) the number *n* of control signals was larger than the number of muscles; *2*) each control was defined by a fixed synergy of muscles; and *3*) the *s* synergies were uniformly distributed in muscular space. Formally, the problem was similar to the problem defined by *Eqs. 5*, *6*, and *7* with the
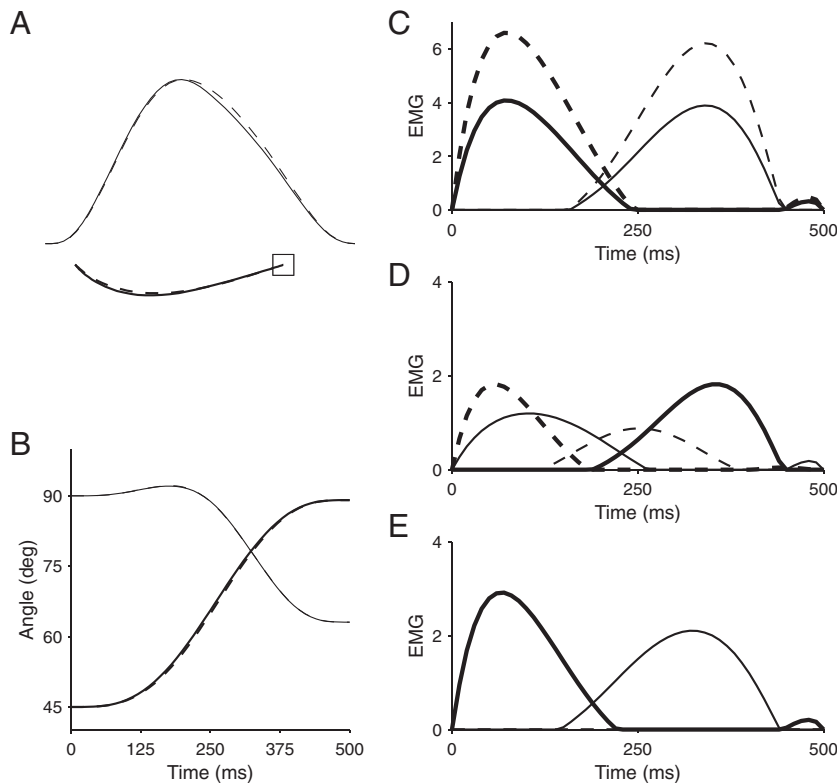
FIG. 10. Influence of biarticular muscles for movements of a planar 2-link arm. *A*: simulation of a 30-cm, leftward, 500-ms movement (*inset*). Normalized velocity profiles are shown. Plain line: model with biarticular muscles. Dashed line: model without biarticular muscles. *B*: angular trajectories (thick: shoulder angle; thin: elbow angle). *C*: EMG in shoulder flexor (thick) and shoulder extensor (thin). *D*: EMG in elbow flexor (thick) and elbow extensor (thin). Elbow flexor is agonist in the absence of biarticular muscles and antagonist in the presence of biarticular muscles. *E*: EMG in biarticular flexor (thick) and extensor (thin) muscles.

following change. The goal was to find minimum controls $\mathbf{U}(t) = \{U_j(t)\}$ ($1 \leq j \leq s$) such that the controls $\{u_i(t)\}$ ($1 \leq i \leq 2N$), defined by

$$u_i(t) = \sum_{j=1 \cdots s} \beta_{ij} U_i(t)$$

where β_{ij} are random coefficients drawn from a uniform distribution in $[-1; 1]$ are appropriate to displace the articulated segments between given initial and final positions. Simulations did not reveal any qualitative differences between synergistic ($s = 500$) and direct ($s = 2N$) control.

DISCUSSION

A proper solution to the *degrees of freedom problem* should be able to explain *1*) how a unique solution is chosen for each realization of a motor act and *2*) why this solution is different each time. The central idea implicit in the proposal of Bernstein and explicitly formulated by Todorov and Jordan (2002) is that the nervous system continuously and efficiently tracks a goal rather than a desired trajectory. This idea was expressed here by two principles (*optimal feedback control* and *maximum efficiency*). We have shown that these two principles combined with a *separation principle* for static and dynamic forces lead
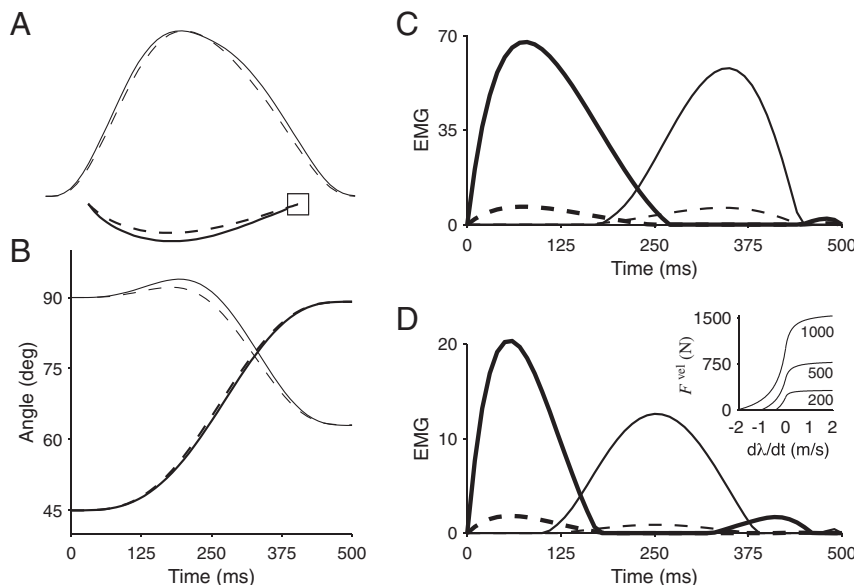

FIG. 11. Influence of force/velocity relationship in muscles for movements of a planar 2-link arm. *A*: simulation of a 30-cm, leftward, 500-ms movement (*inset*). Normalized velocity profiles are shown. Plain line: model with nonlinear muscles. Dashed line: model with linear muscles. *B*: angular trajectories (thick: shoulder angle; thin: elbow angle). *C*: EMG in shoulder flexor (thick) and shoulder extensor (thin). *D*: EMG in elbow flexor (thick) and elbow extensor (thin). *Inset*: velocity-modulated muscle force (F^{vel}) as a function of the rate of change of muscle length (dl/dt) for different levels of maximal isometric for (F^{iso}).

to a realistic solution to redundancy. A fourth principle was added (*constant effort*), which is not directly related to redundancy, to obtain a complete framework.

Limitations

The model has been used to reproduce a wide range of data and we have not found critical discrepancies between experimental observations and predictions of the model—nevertheless, some data cannot be reproduced with the model. Some studies reported nonsymmetric velocity profiles (Brown and Cooke 1990; Gielen et al. 1985) that are not fully explained by the model. Cooke (1980) showed that the slope of amplitude/duration scaling depends on instructions given to the subjects (see also Brown et al. 1990). There is no explanation for this effect in the model. More generally, a weakness of the model is related to its application to highly simplified biomechanical structures. By construction, the biomechanical models are invariant by rotation around the shoulder axis and cannot address the possible influence of position of the arm relative to the body. Furthermore, joints' excursion limits are not represented in the model and it is unclear how movements could be programmed taking these limits into account. An open question is whether the minimum effort principle can be sufficient to penalize movements involving extreme joint configurations. It would render the model much less general if a specific principle was necessary to handle the excursion limits.

Remarks on Bernstein's problem

An important contention of Bernstein is the fact that muscles are not ideal force generators and thus there is no fixed relation between muscle afferent signals and generated muscle force. It might seem paradoxical that we addressed Bernstein's problem by using pure force generators. However, the fact that many factors (such as length, velocity, fatigue, history of activation, etc.) influence the generation of muscle force has no incidence on the proposed solution to kinematic redundancy. We illustrated this issue for velocity-dependent modulation of muscle force in the case where the controller takes this modulation into account. A complementary case is when unpredictable modulations occur (e.g., arising from noise). This condition should be appropriately handled through feedback control (Todorov and Jordan 2002).

Optimal control approach to redundancy

The central tenet of optimal control is that a unique solution to a problem with infinitely many solutions can be obtained in a principled way (Todorov 2004). It is thus not really surprising that kinematic redundancy can be solved in this framework (e.g., Anderson and Pandy 2001). However, the fact that properties of the solution match experimental results for several kinematic chains is not trivial and was not demonstrated before. The main difficulty of the optimal control approach to motor control is that many different models (i.e., many different *cost functions*) can account for properties of movements and it has proven a difficult problem to decide which model is superior to others. In fact, a majority of these models were limited to the explanation of invariant kinematic and dynamic features of movements (e.g., bell-shaped velocity profiles, triphasic EMG). Because of their restricted scope, they could

neither be falsified nor improved based on more integrated characteristics of motor behavior. To evolve from this situation, Harris and Wolpert (1998) and later Todorov and Jordan (2002) proposed that models that encompass a broader range of motor functions should be considered. They introduced behaviorally based cost functions such as the variance of final movement position (Harris and Wolpert 1998) and the trade-off between effort and error (Todorov and Jordan 2002), which account not only for invariant properties of motor control, but also for speed–accuracy trade-off and the structure of motor variability. Our model was designed in this framework and is on the surface similar to these models. The present results extend the relevance of these cost functions to the control of nonlinear kinematically redundant systems.

The model has been applied to several redundant kinematic chains involving the arm. Although the work remains to be done, the model should likely apply to other kinematic chains (e.g., trunk, whole body, orofacial system, digits; Cole and Abbs 1986; Kaminski et al. 1995; Kelso et al. 1985; Pozzo et al. 2002). In fact, the model is consistent with the idea that characteristics of motor behavior (e.g., invariance, covariations, etc.) are related to task constraints and not to specific control parameters (Cole and Abbs 1986).

Other approaches to kinematic redundancy were previously proposed in the literature. Quantitative analyses of redundant movements revealed constraints in movement execution that could contribute to reduce the apparent number of degrees of freedom to be managed by the nervous system (Gielen et al. 1997; Marotta et al. 2003; Medendorp et al. 2000). Yet they have not disclosed origins of these constraints and thus the way redundancy is solved is by the nervous system. Models that addressed kinematic redundancy were customarily concerned with inverse kinematics (Rosenbaum et al. 1995; Torres and Zipser 2002) and thus failed to consider the entire problem encountered by the nervous system.

Separation principle

Several separation principles were proposed in the motor control literature. In the framework of equilibrium-point models, reciprocal (R) activation and coactivation (C) of antagonist muscles operate simultaneously and independently (Feldman and Levin 1995). The R command specifies terminal equilibrium position and the rate of shift toward this equilibrium; the C command sets the level of cocontraction between the muscles. Both commands contribute to posture and movement (Flanagan et al. 1993). Thus separation in this framework is not related to separate static/dynamic control. Separation of inverse dynamics and impedance control was proposed in the framework of internal models (Franklin et al. 2003; Osu et al. 2002, 2003; Takahashi et al. 2001). Accordingly, the motor command would be the sum of *1*) a feedforward command that creates appropriate joint torques to displace the limb along the desired trajectory and *2*) a feedback command that exploits viscoelastic properties of muscles to maintain the correct trajectory despite perturbations. For instance, in an unstable force field, the feedback command is modified to account for the structure of the instability, whereas the feedforward command remains unchanged (Burdet et al. 2001; Franklin et al. 2003). The main limitation of this idea is the tuning of motor commands to a desired trajectory (Todorov and Jordan 2002).

Our separation principle is neither a separation of feedforward and feedback commands nor a separation of reciprocal activation and coactivation. The dynamic command contains both feedforward and feedback components because it results from optimal feedback control. Furthermore, as the dynamic command tracks the goal of the movement, it is not attached to a precomputed trajectory. The function of the static command is to compensate for static forces, i.e., to specify the maintenance of static equilibrium. However, because this controller is a simple mapping between states and forces (see *Eq. 3*), it cannot directly contribute to the stability of the equilibrium. Two ideas have been proposed to explain how the nervous system tackles equilibrium and stability. The first is the notion of impedance controller, i.e., a controller that exploits viscoelastic properties of muscles to maintain stable equilibrium despite perturbations (Burdet et al. 2001; Darainy et al. 2004; Franklin et al. 2003). However, the viscoelastic properties of muscles may not be appropriate to guarantee stability (Dornay et al. 1993; Loram and Lakie 2002; Morasso and Schieppati 1999; Shadmehr and Arbib 1992). The second idea is based on the notion that postural maintenance would be an active state subject to anticipatory control rather than a passive state subject to reactive control (Loram et al. 2001; Morasso and Sanguineti 2002; Morasso and Schieppati 1999). In this case, a basic static controller (state/force mapping) could be sufficient, postural maintenance being subserved by the dynamic controller (Loram et al. 2005). This scenario has been found to be efficient in the linear case (Fig. 1*D*) and would need to be extended to the nonlinear case.

The neural bases for a separation principle are still elusive. We first note that our separation principle is consistent with, but more general than, a separation of reciprocal activation and coactivation (De Luca and Mambrito 1987; Humphrey and Reed 1983). At the cortical level, putative correlates of static and dynamic controls were previously described in primate primary motor cortex as tonic and phasic-tonic patterns of discharge (Kalaska et al. 1989; Sergio and Kalaska 1998; Sergio et al. 2005). However, other types of discharge have been reported that could be considered to contradict the separation principle (Cheney and Fetz 1980; Kalaska et al. 1989; Kurtzer et al. 2005b). At the spinal level, it is expected that the two commands are additive, i.e., the force generated in a muscle by the sum of the commands is the sum of the forces generated by each command. Although additivity has been observed in some circumstances (Farley and Koshland 2000; Rimmer et al. 1995; Sergio and Ostry 1994, 1995), it may not be a general case because of the threshold behavior in motoneurons.

Constant effort principle

This principle was introduced to translate verbal instructions into motor operations. It specifies the level of effort necessary to build the dynamic forces required to execute a movement of a given amplitude. In this way, movement time is implicitly determined by a scaling law (Fig. 8*B*). A consequence of this principle is *kinematic invariance*, which refers to the use of a single velocity profile scaled in time and amplitude when movements of different amplitudes or against different inertial loads are performed. Scaling in time and amplitude results from adjustments in movement time required to match the

desired level of effort. There is no principled explanation of this property in current models of motor control. In particular, the idea that kinematic invariance would result from movement specification at a kinematic level has been challenged (Todorov and Jordan 2002). The constant effort principle also explains directional variations in movement time, peak velocity, and peak accelerations as variations resulting from the shape of the inertia matrix of the moving limb (Gordon et al. 1994; Pellegrini and Flanders 1996; Turner et al. 1995). This interpretation competes with the proposal that the nervous system fails to compensate for the inertial anisotropy of the arm (Gordon et al. 1994; for a model see Todorov 1998) and is more compatible with data showing that inertial properties of the limb are taken into account for trajectory formation (Flanagan and Lolley 2001; Gentili et al. 2004; Sabes et al. 1998).

The constant effort principle applies to dynamic forces. It is unclear whether a similar principle applies to static forces (Klein Breteler et al. 2003; Nishikawa et al. 1999). The model gives no rules with which to specify a "natural" static effort level (e.g., level of cocontraction) associated with a given movement. It is possible that there is a coupling between static and dynamic efforts, i.e., the nervous system simultaneously allots effort for static and dynamic forces. This issue could be addressed by measuring cocontraction levels (e.g., Gribble et al. 2003) during movements of increasing amplitude. It was previously shown that cocontraction increases with velocity (Gribble and Ostry 1998; Suzuki et al. 2001).

A question is why the nervous system would specify a level of effort rather than a duration. It is clear that the nervous system can finely manipulate the timing of motor actions (Schöner 2002). However, amplitude-, load-, and direction-dependent variations in movement duration are not easily explained in this framework. Effort is an interesting parameter because it somewhat reflects physical energy consumption. Thus the choice of an effort level can be dictated by available resources (such as level of fatigue) and required/expected expenditures (such as number of movements to execute).

Finally, we note that, even if one does not adhere to the constant effort principle, the results related to kinematic redundancy remain valid.

Neural bases of the model

Although the model was described at a computational level, it can be related to neural components of motor control. The muscles were represented by a second-order nonlinear filter (*Eq. 4*) and their excitation level can be related to electromyographic signals. As expected, excitation exhibited a triphasic agonist/antagonist pattern (see Fig. 9*D*) as classically reported in the literature for fast movements. The control signals can be considered as inputs to motoneurons (*Eq. 4*) and could thus correspond to activities in subsets of cortical and spinal neurons. Because the control signals are completely responsible for the temporal profile of excitation, they should exhibit an early phasic component followed by a depression for movements in a given direction and a delayed phasic component for movements in the opposite direction. In fact, they should resemble the discharge pattern of EMG-like neurons found in primate motor cortex (Sergio and Kalaska 1998; Sergio et al. 2005). If we accept this idea, the model suggests that the motor cortex contains an inverse model of the neuromuscular appa-

ratus. This view concurs with a recent computational model showing that many correlations between kinematic quantities and neural discharges in motor cortex can be explained by the hypothesis that motor cortical neurons calculate muscular activation patterns (Todorov 2000). In this framework, the model further suggests that computation at the muscular level in motor cortex could be directly responsible for the production of kinematically realistic movements. More generally the model contributes to the hotly debated issue of the neural representation of movement in motor cortical regions (Georgopoulos and Ashe 2000; Graziano 2006; Moran and Schwartz 2000; Todorov 2000, 2003).

Can this model be of interest for experimentalists?

It is interesting to ask whether this model can be useful to researchers involved in the study of motor control. We strongly believe that it should be the case, in particular to put constraints on the interpretation of experimental observations. We provide two examples. The first is a general issue related to the nature and origin of motor invariants. The existence of motor invariants is generally thought to reflect a requirement elaborated by the nervous system; e.g., hand velocity has a bell-shaped profile because it corresponds to a kind of desired or desirable profile. The model suggests an alternative interpretation because invariants can also be found in the absence of reference trajectory. Thus conclusions based on the observation of motor invariants should be made cautiously with due consideration to different proposals. The second is a specific example related to the interpretation of an experimental result. Sober and Sabes (2003) observed that initial movement directions of planar pointing movements deviated systematically from target direction when vision and proprioception were dissociated, i.e., subjects received a wrong visual feedback of the position of their hand. These authors provided an explanation of the pattern of error based on the idea that both proprioception and vision contribute to the estimation of hand position, i.e., the hand is felt to be somewhere between its visual image and its true proprioceptive location. Errors arise because motor commands are computed using the felt rather than the true position. The present model can be used to simulate the experiment of Sober and Sabes (2003). We simulated movements toward eight targets arrayed on a circle under three conditions (Fig. 12A): *1*) initial hand position is at the center of the circle and is actually seen at this position (baseline); *2*) visual feedback of the hand is shifted to the left; and *3*) visual feedback of the hand is shifted to the right. We assumed that the movement vector is the vector from the visual hand to the target (Fig. 12A). We measured initial movement directions for the three conditions and we calculated errors resulting from shift in visual feedback by subtracting errors in the baseline condition (Fig. 12B). Then we fitted the velocity command model of Sober and Sabes (2003) to our data, i.e., we searched for the estimated hand position that best explains the pattern of errors (Fig. 12B). We found that (see Fig. 12A for notations)

$$x_{estimated} = 0.35x_{vis} + 0.65x_{prop}$$

which is close to the fit obtained by Sober and Sabes (2003). Thus a possible interpretation of this experiment is that initial direction errors result from an imperfect control applied at the true hand position (our model) rather than
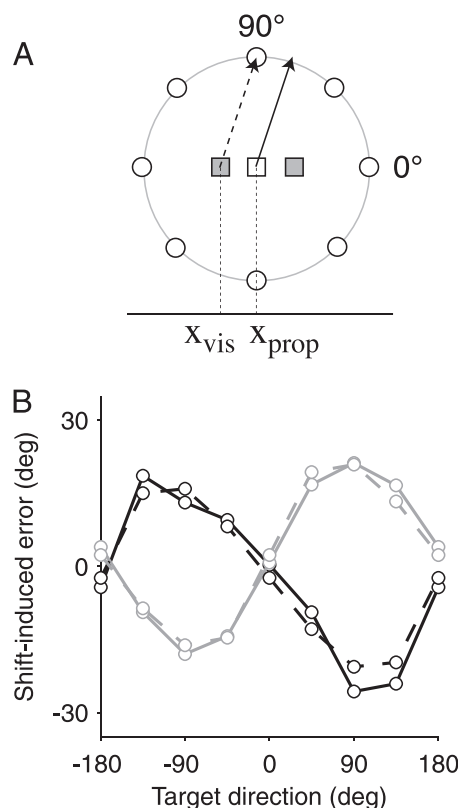

FIG. 12. Simulation of the experiment of Sober and Sabes (2003). *A*: experimental paradigm. Initial hand position is represented by an open square and targets by circles (distance is 18 cm). Gray squares: shifted visual feedback of initial hand position (to left or to the right). Dashed arrow: desired movement vector for a target at 90° when hand is visually shifted to the left. Plain arrow: actual movement vector. Movement duration was 500 ms. *B*: shift-induced errors in initial movement direction (after subtraction of errors in the unshifted condition) as a function of target direction for a left shift (black solid line) and a right shift (gray solid line). Dashed lines: best fit to the data (see text).

from a correct control applied to a wrong hand position (Sober and Sabes' model). These two examples show that the model can provide interesting alternative insights into experimental data.

The model can also generate predictions that could be tested in future experiments (e.g., variations of movement curvature with initial posture and direction, relationship between variations of movement duration for movements in 3D space and arm inertia) and used as further tests of the model.

In conclusion, we have proposed a description of motor behavior, based on four overarching principles, that provides a unique framework to explain behavioral characteristics of point-to-point movements with a parameter-free model. The model provides a quantitative solution to kinematic redundancy and accounts for kinematic invariance.

REFERENCES

Admiraal MA, Kusters MJ, Gielen SC. Modeling kinematics and dynamics of human arm movements. *Motor Control* 8: 312–338, 2004.

Alexandrov A, Frolov A, Massion J. Axial synergies during human upper trunk bending. *Exp Brain Res* 118: 210–220, 1998.

Anderson FC, Pandy MG. Dynamic optimization of human walking. *J Biomech Eng* 123: 381–390, 2001.

Atkeson CG, Hollerbach JM. Kinematic features of unrestrained vertical arm movements. *J Neurosci* 5: 2318–2330, 1985.

Baddeley RJ, Ingram HA, Miall RC. System identification applied to a visuomotor task: near-optimal human performance in a noisy changing task. *J Neurosci* 23: 3066–3675, 2003.

Bennis N, Roby-Brami A. Coupling between reaching movement direction and hand orientation for grasping. *Brain Res* 952: 257–267, 2002.

Bernstein N. *The Co-ordination and Regulation of Movements.* Oxford, UK: Pergamon Press, 1967.

Bock O. Load compensation in human goal-directed arm movements. *Behav Brain Res* 41: 167–177, 1990.

Brown SH, Cooke JD. Movement-related phasic muscle activation. I. Relations with temporal profile of movement. *J Neurophysiol* 63: 455–464, 1990.

Brown SH, Hefter H, Mertens M, Freund HJ. Disturbances in human arm trajectory due to mild cerebellar dysfunction. *J Neurol Neurosurg Psychiatry* 53: 306–313, 1990.

Bryson AE. *Dynamic Optimization.* Englewood Cliffs, NJ: Prentice Hall, 1999.

Bryson AE, Ho Y-C. *Applied Optimal Control—Optimization, Estimation, and Control.* New York: Hemisphere, 1975.

Bullock D, Grossberg S. Neural dynamics of planned arm movements: emergent invariance and speed-accuracy properties during trajectory formation. *Psychol Rev* 95: 49–90, 1988.

Buneo CA, Soechting JF, Flanders M. Muscle activation patterns for reaching: the representation of distance and time. *J Neurophysiol* 71: 1546–1558, 1994.

Burdet E, Osu R, Franklin DW, Milner TE, Kawato M. The central nervous system stabilizes unstable dynamics by learning optimal impedance. *Nature* 414: 446–449, 2001.

Cheney PD, Fetz EE. Functional classes of primate corticomotoneuronal cells and their relation to active force. *J Neurophysiol* 44: 773–791, 1980.

Cole KJ, Abbs JH. Coordination of three-joint digit movements for rapid finger-thumb grasp. *J Neurophysiol* 55: 1407–1423, 1986.

Cooke JD. The organization of simple skilled movements. In: *Advances in Psychology: Tutorials in Motor Behavior*, edited by Stelmach GE, Requin J. Amsterdam: North-Holland, 1980, p. 199–212.

Cuijpers RH, Smeets JB, Brenner E. On the relation between object shape and grasping kinematics. *J Neurophysiol* 91: 2598–2606, 2004.

Darainy M, Malfait N, Gribble PL, Towhidkhah F, Ostry DJ. Learning to control arm stiffness under static conditions. *J Neurophysiol* 92: 3344–3350, 2004.

De Luca CJ, Mambrito B. Voluntary control of motor units in human antagonist muscles: coactivation and reciprocal activation. *J Neurophysiol* 58: 525–542, 1987.

Desmurget M, Grafton S. Forward modeling allows feedback control for fast reaching movements. *Trends Cogn Sci* 4: 423–431, 2000.

Desmurget M, Gréa H, Prablanc C. Final posture of the upper limb depends on the initial position of the hand during prehension movements. *Exp Brain Res* 119: 511–516, 1998.

Desmurget M, Prablanc C, Arzi M, Rossetti Y, Paulignan Y, Urquizar C. Integrated control of hand transport and orientation during prehension movements. *Exp Brain Res* 110: 265–278, 1996.

Dornay M, Mussa-Ivaldi FA, McIntyre J, Bizzi E. Stability constraints for the distributed control of motor behavior. *Neural Netw* 6: 1045–1059, 1993.

Dornay M, Uno Y, Kawato M, Suzuki R. Minimum muscle tension change trajectories predicted by using a 17-muscle model of the monkey's arm. *J Mot Behav* 28: 83–100, 1996.

Farley BG, Koshland GF. Trunk muscle activity during the simultaneous performance of two motor tasks. *Exp Brain Res* 135: 483–496, 2000.

Feldman AG, Levin MF. The origin and use of positional frames of reference in motor control. *Behav Brain Sci* 18: 723–744, 1995.

Fernandez L, Bootsma RJ. Effects of biomechanical and task constraints on the organization of movement in precision aiming. *Exp Brain Res* 159: 458–466, 2004.

Fitts PM. The information capacity of the human motor system in controlling the amplitude of movement. *J Exp Psychol* 47: 381–391, 1954.

Flanagan JR, Lolley S. The inertial anisotropy of the arm is accurately predicted during movement planning. *J Neurosci* 21: 1361–1369, 2001.

Flanagan JR, Ostry DJ, Feldman AG. Control of trajectory modifications in target-directed reaching. *J Mot Behav* 25: 140–152, 1993.

Flanders M, Daghestani L, Berthoz A. Reaching beyond reach. *Exp Brain Res* 126: 19–30, 1999.

Flanders M, Herrmann U. Two components of muscle activation: scaling with the speed of arm movement. *J Neurophysiol* 67: 931–943, 1992.

Flanders M, Pellegrini JJ, Geisler SD. Basic features of phasic activation for reaching in vertical planes. *Exp Brain Res* 110: 67–79, 1996.

Flash T. The organization of human arm trajectory control. In: *Multiple Muscle Systems: Biomechanics and Movement Organization*, edited by Winters JM, Woo SL-Y. New York: Springer-Verlag, 1990, p. 282–301.

Flash T. Arm movement and stiffness adaptation to external loads. *Proc IEEE Eng Med Biol Conf* 13: 885–886, 1992.

Flash T, Hogan N. The coordination of arm movements: an experimentally confirmed mathematical model. *J Neurosci* 5: 1688–1703, 1985.

Franklin DW, Osu R, Burdet E, Kawato M, Milner TE. Adaptation to stable and unstable dynamics achieved by combined impedance control and inverse dynamics model. *J Neurophysiol* 90: 3270–3282, 2003.

Gentili R, Cahouet V, Ballay Y, Papaxanthis C. Inertial properties of the arm are accurately predicted during motor imagery. *Behav Brain Res* 155: 231–239, 2004.

Gentner DR. Timing of skilled motor performance: tests of the proportional duration model. *Psychol Rev* 94: 255–276, 1987.

Georgopoulos AP, Ashe J. One motor cortex, two different views. *Nat Neurosci* 3: 963, 2000.

Ghez C. Contributions of central programs to rapid limb movement in the cat. In: *Integration in the Nervous System*, edited by Asanuma H, Wilson VJ. Tokyo: Igaku-Shoin, 1979, p. 305–320.

Gielen CCAM, van Bolhuis BM, Theeuwen M. On the control of biologically and kinematically redundant manipulators. *Hum Mov Sci* 14: 487–509, 1995.

Gielen CCAM, van den Oosten K, Pul ter Gunne F. Relation between EMG activation patterns and kinematic properties of aimed arm movements. *J Mot Behav* 17: 421–442, 1985.

Gielen CCAM, Vrijenhoek EJ, Flash T, Neggers SFW. Arm position constraints during pointing and reaching in 3-D space. *J Neurophysiol* 78: 660–673, 1997.

Gordon J, Ghilardi MF, Cooper SE, Ghez C. Accuracy of planar reaching movements. II. Systematic extent errors resulting from inertial anisotropy. *Exp Brain Res* 99: 112–130, 1994.

Gottlieb GL. On the voluntary movement of compliant (inertial-viscoelastic) loads by parcellated control mechanisms. *J Neurophysiol* 76: 3207–3229, 1996.

Gottlieb GL, Song QL, Almeida GL, Hong DA, Corcos DM. Directional control of planar human arm movement. *J Neurophysiol* 78: 2985–2998, 1997.

Graziano M. The organization of behavioral repertoire in motor cortex. *Annu Rev Neurosci* 29: 105–134, 2006.

Gribble PL, Mullin LI, Cothros N, Mattar A. Role of cocontraction in arm movement accuracy. *J Neurophysiol* 89: 2396–2405, 2003.

Gribble PL, Ostry DJ. Independent coactivation of shoulder and elbow muscles. *Exp Brain Res* 123: 355–360, 1998.

Happee R. Goal-directed arm movements. III. Feedback and adaptation in response to inertial perturbations. *J Electromyogr Kinesiol* 3: 112–122, 1993.

Harris CM, Wolpert DM. Signal-dependent noise determines motor planning. *Nature* 394: 780–784, 1998.

Hatzitaki V, McKinley P. Effect of single-limb inertial loading on bilateral reaching: interlimb interactions. *Exp Brain Res* 140: 34–45, 2001.

Hermens F, Gielen S. Posture-based or trajectory-based movement planning: a comparison of direct and indirect pointing movements. *Exp Brain Res* 159: 340–348, 2004.

Hoff B, Arbib MA. Models of trajectory formation and temporal interaction of reach and grasp. *J Mot Behav* 25: 175–192, 1993.

Hogan N. An organizing principle for a class of voluntary movements. *J Neurosci* 4: 2745–2754, 1984.

Humphrey DR, Reed DJ. Separate cortical systems for control of joint movement and joint stiffness: reciprocal activation and coactivation of antagonist muscles. In: *Motor Control Mechanisms in Health and Disease*, edited by Desmedt JE. New York: Raven Press, 1983, p. 347–372.

Jagacinski RJ, Monk DL. Fitts' law in two dimensions with hand and head movements. *J Mot Behav* 17: 77–95, 1985.

Kalaska JF, Cohen DAD, Hyde ML, Prud'homme M. A comparison of movement direction-related versus load direction-related activity in primate motor cortex, using a two-dimensional reaching task. *J Neurosci* 9: 2080–2102, 1989.

Kaminski TR, Bock C, Gentile AM. The coordination between trunk and arm motion during pointing movements. *Exp Brain Res* 106: 457–466, 1995.

Kaminski TR, Gentile AM. A kinematic comparison of single and multijoint pointing movements. *Exp Brain Res* 78: 547–556, 1989.

Kelso JAS, Vatikiotis-Bateson E, Saltzman EL, Kay B. A qualitative dynamic analysis of reiterant speech production: phase portraits, kinematics, and dynamic modeling. *J Acoust Soc Am* 77: 266–280, 1985.

Kirk DE. *Optimal Control Theory.* Englewood Cliffs, NJ: Prentice-Hall, 1970.

Klein Breteler MD, Hondzinski JM, Flanders M. Drawing sequences of segments in 3D: kinetic influences on arm configuration. *J Neurophysiol* 89: 3253–3263, 2003.

Klein Breteler MD, Meulenbroek RG, Gielen CCAM. Geometric features of workspace and joint-space paths of 3D reaching movements. *Acta Psychol (Amst)* 100: 37–53, 1998.

Kuo AD. An optimal-control model for analyzing postural balance. *IEEE Trans Biomed Eng* 42: 87–101, 1995.

Kurtzer I, DiZio PA, Lackner JR. Adaptation to a novel multi-force environment. *Exp Brain Res* 164: 120–132, 2005a.

Kurtzer I, Herter TM, Scott SH. Random change in cortical load representation suggests distinct control of posture and movement. *Nat Neurosci* 8: 498–504, 2005b.

Lashley KS. Integrative function of the cerebral cortex. *Physiol Rev* 13: 1–42, 1933.

Levin O, Wenderoth N, Steyvers M, Swinnen SP. Directional invariance during loading-related modulations of muscle activity: evidence for motor equivalence. *Exp Brain Res* 148: 62–76, 2003.

Loram ID, Kelly SM, Lakie M. Human balancing of an inverted pendulum: is sway size controlled by ankle impedance? *J Physiol* 532: 879–891, 2001.

Loram ID, Lakie M. Direct measurement of human ankle stiffness during quiet standing: the intrinsic mechanical stiffness is insufficient for stability. *J Physiol* 545: 1041–1053, 2002.

Loram ID, Maganaris CN, Lakie M. Human postural sway results from frequent, ballistic bias impulses by soleus and gastrocnemius. *J Physiol* 564: 295–311, 2005.

Marotta JJ, Medendorp WP, Crawford JD. Kinematic rules for upper and lower arm contributions to grasp orientation. *J Neurophysiol* 90: 3816–3827, 2003.

Medendorp WP, Crawford JD, Henriques DY, Van Gisbergen JA, Gielen CC. Kinematic strategies for upper arm-forearm coordination in three dimensions. *J Neurophysiol* 84: 2302–2316, 2000.

Milner TE. Adaptation to destabilizing dynamics by means of muscle cocontraction. *Exp Brain Res* 143: 406–416, 2002.

Moran DW, Schwartz AB. One motor cortex, two different views (Letter). *Nat Neurosci* 3: 963, 2000.

Morasso PG, Sanguineti V. Ankle muscle stiffness alone cannot stabilize balance during quiet standing. *J Neurophysiol* 88: 2157–2162, 2002.

Morasso PG, Schieppati M. Can muscle stiffness alone stabilize upright standing? *J Neurophysiol* 82: 1622–1626, 1999.

Murata A, Iwase H. Extending Fitts' law to a three-dimensional pointing task. *Hum Mov Sci* 20: 791–805, 2001.

Mustard BE, Lee RG. Relationship between EMG patterns and kinematic properties for flexion movements at the human wrist. *Exp Brain Res* 66: 247–256, 1987.

Nelson WL. Physical principles for economies of skilled movements. *Biol Cybern* 46: 135–147, 1983.

Nishikawa KC, Murray ST, Flanders M. Do arm postures vary with the speed of reaching? *J Neurophysiol* 81: 2582–2586, 1999.

Ostry DJ, Cooke JD, Munhall KG. Velocity curves of human arm and speech movements. *Exp Brain Res* 68: 37–46, 1987.

Osu R, Burdet E, Franklin DW, Milner TE, Kawato M. Different mechanisms involved in adaptation to stable and unstable dynamics. *J Neurophysiol* 90: 3255–3269, 2003.

Osu R, Franklin DW, Kato H, Gomi H, Domen K, Yoshioka T, Kawato M. Short- and long-term changes in joint co-contraction associated with motor learning as revealed from surface EMG. *J Neurophysiol* 88: 991–1004, 2002.

Papaxanthis C, Pozzo T, Schieppati M. Trajectories of arm pointing movements on the sagittal plane vary with both direction and speed. *Exp Brain Res* 148: 498–503, 2003.

Pellegrini JJ, Flanders M. Force path curvature and conserved features of muscle activation. *Exp Brain Res* 110: 80–90, 1996.

Pozzo T, Stapley PJ, Papaxanthis C. Coordination between equilibrium and hand trajectories during whole body pointing movements. *Exp Brain Res* 144: 343–350, 2002.

Rand MK, Shimansky Y, Stelmach GE, Bloedel JR. Adaptation of reach-to-grasp movement in response to force perturbations. *Exp Brain Res* 154: 50–65, 2004.

Rimmer KP, Ford GT, Whitelaw WA. Interaction between postural and respiratory control of human intercostal muscles. *J Appl Physiol* 79: 1556–1561, 1995.

Roby-Brami A, Bennis N, Mokhtari M, Baraduc P. Hand orientation for grasping depends on the direction of the reaching movement. *Brain Res* 869: 121–129, 2000.

Rosenbaum DA, Loukopoulos LD, Meulenbroek RGJ, Vaughan J, Engelbrecht SE. Planning reaches by evaluating stored postures. *Psychol Rev* 102: 28–67, 1995.

Ruitenbeek JC. Invariants in loaded goal directed movements. *Biol Cybern* 51: 11–20, 1984.

Sabes PN, Jordan MI, Wolpert DM. The role of inertial sensitivity in motor planning. *J Neurosci* 18: 5948–5957, 1998.

Schöner G. Timing, clocks, and dynamical systems. *Brain Cogn* 48: 31–51, 2002.

Sergio LE, Hamel-Paquet C, Kalaska JF. Motor cortex neural correlates of output kinematics and kinetics during isometric-force and arm-reaching tasks. *J Neurophysiol* 94: 2353–2378, 2005.

Sergio LE, Kalaska JF. Changes in the temporal pattern of primary motor cortex activity in a directional isometric force versus limb movement task. *J Neurophysiol* 80: 1577–1583, 1998.

Sergio LE, Ostry DJ. Coordination of mono- and bi-articular muscles in multi-degree of freedom elbow movements. *Exp Brain Res* 97: 551–555, 1994.

Sergio LE, Ostry DJ. Coordination of multiple muscles in two degree of freedom elbow movements. *Exp Brain Res* 105: 123–137, 1995.

Shadmehr R, Arbib MA. A mathematical analysis of the force-stiffness characteristics of muscles in control of a single joint system. *Biol Cybern* 66: 463–477, 1992.

Shadmehr R, Moussavi ZM. Spatial generalization from learning dynamics of reaching movements. *J Neurosci* 20: 7807–7815, 2000.

Shadmehr R, Mussa-Ivaldi FA. Adaptive representation of dynamics during learning a motor task. *J Neurosci* 14: 3208–3224, 1994.

Smyrnis N, Evdokimidis I, Constantinidis TS, Kastrinakis G. Speed-accuracy trade-off in the performance of pointing movements in different directions in two-dimensional space. *Exp Brain Res* 134: 21–31, 2000.

Sober SJ, Sabes PN. Multisensory integration during motor planning. *J Neurosci* 23: 6982–6992, 2003.

Soechting JF, Buneo CA, Herrmann U, Flanders M. Moving effortlessly in three dimensions: does Donders' law apply to arm movement? *J Neurosci* 15: 6271–6280, 1995.

Soechting JF, Flanders M. Movement planning: kinematics, dynamics, both or neither? In: *Vision and Action*, edited by Harris LR, Jenkin M. Cambridge, UK: Cambridge Univ. Press, 1998, p. 332–349.

Soechting JF, Lacquaniti F. Invariant characteristics of a pointing movement in man. *J Neurosci* 1: 710–720, 1981.

Spong MS, Vidyasagar M. *Robot Dynamics and Control.* New York: Wiley, 1989.

Sporns O, Edelman GM. Solving Bernstein's problem: a proposal for the development of coordinated movement by selection. *Child Dev* 64: 960–981, 1993.

Suzuki M, Shiller DM, Gribble PL, Ostry DJ. Relationship between cocontraction, movement kinematics and phasic muscle activity in single-joint arm movement. *Exp Brain Res* 140: 171–181, 2001.

Takahashi CD, Scheidt RA, Reinkensmeyer DJ. Impedance control and internal model formation when reaching in a randomly varying dynamical environment. *J Neurophysiol* 86: 1047–1051, 2001.

Thoroughman KA, Feller KJ. Gravitational effects on torque change and variance optimization in reaching movements. Program No. 492.20. *2003 Abstract Viewer/Itinerary Planner.* Washington, DC: Society for Neuroscience, 2003, Online.

Todorov E. *Studies of Goal-Directed Movements* (PhD dissertation, unpublished). Cambridge, MA: Massachusetts Institute of Technology, 1998.

Todorov E. Direct cortical control of muscle activation in voluntary arm movements: a model. *Nat Neurosci* 3: 391–398, 2000.

Todorov E. On the role of primary motor cortex in arm movement control. In: *Progress in Motor Control III*, edited by Latash ML, Levin MF. Champaign, IL: Human Kinetics, 2003, p. 125–166.

Todorov E. Optimality principles in sensorimotor control. *Nat Neurosci* 7: 907–915, 2004.

Todorov E, Jordan MI. Optimal feedback control as a theory of motor coordination. *Nat Neurosci* 5: 1226–1235, 2002.

Torres EB, Zipser D. Reaching to grasp with a multi-jointed arm. I. Computational model. *J Neurophysiol* 88: 2355–2367, 2002.

Torres EB, Zipser D. Simultaneous control of hand displacements and rotations in orientation-matching experiments. *J Appl Physiol* 96: 1978–1987, 2004.

Turner RS, Owens JWM, Anderson ME. Directional variation of spatial and temporal characteristics of limb movements made by monkeys in a two-dimensional work space. *J Neurophysiol* 74: 684–697, 1995.

Uno Y, Kawato M, Suzuki R. Formation and control of optimal trajectory in human multijoint arm movement—minimum torque change model. *Biol Cybern* 61: 89–101, 1989.

van der Helm FCT, Rozendaal LA. Musculoskeletal systems with intrinsic and proprioceptive feedback. In: *Biomechanics and Neural Control of Posture and Movement*, edited by Winters JM, Crago PE. New York: Springer-Verlag, 2000, p. 164–174.

Virji-Babul N, Cooke JD, Brown SH. Effects of gravitational forces on single joint arm movements in human. *Exp Brain Res* 99: 338–346, 1994.

Welter TG, Bobbert MF. Initial muscle activity in planar ballistic arm movements with varying external force directions. *Motor Control* 6: 32–51, 2002.

Wolpert DM, Ghahramani Z, Jordan MI. An internal model for sensori-motor integration. *Science* 269: 1880–1882, 1995.

Zelaznik HN, Schmidt RA, Gielen CCAM. Kinematic properties of rapid aimed hand movements. *J Mot Behav* 18: 353–372, 1986.

Zhang X, Chaffin DB. The effects of speed variation on joint kinematics during multisegment reaching movements. *Hum Mov Sci* 18: 741–757, 1999.